LOS ALAMOS NATIONAL LABORATORY
LA-UR-02-4979

DRAFT

# THEORY AND TECHNIQUE OF BEAM ENVELOPE SIMULATION

## SECOND EDITION

## SIMULATION OF BUNCHED PARTICLE BEAMS WITH ELLIPSOIDAL SYMMETRY AND LINEAR SPACE CHARGE FORCES

Christopher K. Allen
*Los Alamos National Laboratory*
*Los Alamos, New Mexico*

## Table of Contents

*1. Introduction* ____ *4*
1.1. Overview ____ 4
1.2. Outline ____ 5
*2. Physics Background* ____ *5*
2.1. The Design Trajectory ____ 5
2.2. Phase Space ____ 6
2.3. Homogeneous Coordinates ____ 6
2.4. The Longitudinal Phase Plane ____ 7
2.5. Equations of Motion ____ 8
*3. Statistics Background* ____ *10*
3.1. The Density Function ____ 10
3.2. Liouville's Theorem ____ 10
3.3. Moments of the Distribution ____ 11
3.4. Moment Equations ____ 11
*4. Beam Physics* ____ *12*
4.1. The RMS Envelopes ____ 12
4.2. RMS Emittance ____ 13
4.3. Courant-Snyder Parameters for the RMS Ellipse ____ 15
4.4. The Mean Value Vector and Correlation Matrix ____ 16
4.5. The Covariance Matrix and Courant-Snyder Relations ____ 17
4.6. Linearization of the Self-Fields ____ 18
4.7. Tune Depression ____ 19
*5. Ellipsoidal Beams and the Equivalent Uniform Beam* ____ *20*
5.1. Ellipsoidally Symmetric Charge Density Distributions ____ 20
5.2. Arbitrarily Oriented Ellipsoidal Charge Densities ____ 21
5.3. Ellipsoidally Symmetric Phase Space Distributions ____ 23
5.4. Computation of the Field Moments ____ 24
5.5. The Equivalent Uniform Beam ____ 25
*6. Bunched Beam Envelope Equations* ____ *27*
6.1. Equations for Centroid Motion ____ 27
6.2. Bunched Beam RMS Envelope Equations ____ 28
6.3. Ellipsoidally Symmetric Beams and the Equivalent Uniform Beam ____ 28
6.4. Approximate Form of the Envelope Equations ____ 29
*7. Transfer Matrix Approach* ____ *31*
7.1. Transfer Matrices and External Elements ____ 32
7.2. Space Charge Impulses ____ 33

**7.3. Space Charge Defocal Lengths** 34
**7.4. Equations for Centroid Motion** 36
**7.5. Equations for the Second-Order Moments** 36
**7.6. Extensions to the Inhomogeneous Case** 37
**7.7. Homogeneous Coordinates** 38
***8. Summary and Conclusion*** *39*
***Acknowledgements*** *40*
***Appendix A: Transfer Matrices for Common Beamline Elements*** *41*
**A.1 Drift Space** 41
**A.2 Quadrupole** 41
**A.3 Dipole Steering Magnet (As a Thin Lens)** 42
**A.4 Dipole Steering Magnet (As a Thick Lens)** 42
**A.5 Bending Magnet** 44
**A.6 RF Gap (As a Thin Lens)** 46
***Appendix B: 2D Phase Space Moment Calculations*** *48*
***Appendix B: Notes on the Special Orthogonal Groups SO(2) and SO(3)*** *49*
***Appendix C: Self-Field Moment Calculation*** *51*
***References*** *53*

# 1. INTRODUCTION

A convenient way to describe particle beam behavior is through the use of statistics. For instance, instead of a full multiple-particle simulation we can propagate the statistical properties of the beam down the beamline, such as its various statistical moments. Of course such an approach does not provide as much information as a multiple-particle simulation, however, it is computationally much less expensive. The approach is that taken by the simulation codes TRANSPORT [4] and TRACE3D [7]. The current note describes this type of simulation technique in some detail, in particular, the beam physics background, computation of the self-force effects on the dynamics (i.e., space charge effects), and numerical approaches.

It is our intention to describe in some detail the theory and technique for simulation of particle beam envelopes. We hope that this unified presentation will serve as a collective documentation for such techniques that are already in common practice. By fully documenting both the theory and numerical techniques one can more readily develop extensions to the theory and techniques and draw conclusions toward the validity of the resulting simulations. For example, we could extend the theory here to include noise from machine errors, or use the theory included here to determine which regimes the simulations are most accurate. Because our interests are primarily in the control and automation of accelerator systems, it is important to us that we have a clear understanding of the simulation techniques being employed to develop robust control applications. The techniques presented here are fast. Thus, not only are they useful for off-line accelerator system design, they are also valuable for presenting on-line model references for developing control applications.

Although we cover the theory and technique of beam envelope simulation in detail, we mention nothing about how one might actually implement such a simulation engine. In a companion article we present a modern software architecture for performing these simulations [18]. This architecture has already been implemented and is in current use, embedded into the high-level control system for the Spallation Neutron Source (SNS) accelerator.

## 1.1. Overview

We begin with the equations of motion for single particle trajectory under Lorentz forces. These equations are tailored to beam physics by using the path length along the design trajectory as the independent variable, rather than time. By employing Liouville's theorem we find it possible to derive evolution equations for the beam ensemble's moments from the equations for single particle motion. There are two unresolved terms in these equations, both determining the effects of the beam's self fields on the moment dynamics. Specifically, they are the cross-moments of the self electric field and the phase coordinates. If we assume that the beam has ellipsoidal symmetry in configuration space, it is possible to compute one of these moments analytically in terms of elliptic integrals (the moment involving the spatial coordinate). Upon computing this moment we find that it depends only weakly on the actual profile of the ellipsoidal distribution. Acknowledging this fact we typically model all laboratory beams with an equivalent uniform beam having the same second moments; the uniform beam is preferred since it has well-defined boundaries. From there we take two different approaches in the description of the statistical evolution of the beam.

From the moment equations we can derive a convenient set of equations that describe the behavior of the rms beam envelopes (assuming a centered beam). We avoid the remaining unknown field moment by introducing the definition of rms emittance in the equation set. By doing so, however, we implicitly make the assumption that the rms emittance is either constant or it is a function whose values are known a priori. This assumption is usually not too restrictive, since it is known that rms emittances are invariants of the motion if all forces on the beam are linear. The resulting set of equations for rms envelopes can also be rewritten for the equivalent uniform beam, and is usually seen that way in the literature. They form a convenient closed set of equations for studying beam dynamics. However, as pointed out they cannot be used to study nonlinear effects acting on the beam.

The alternate approach to developing a description of the beam's statistical evolution is through the use of transfer matrices. While the previous approach results in a set of coupled ordinary equations that are

continuous in nature, this technique is more of a discrete approach. Generally, the continuous representation is most convenient for analytic study while the discrete representation is well suited for computer simulation. The transfer matrix technique is based upon the observation that whenever all forces on a particle are linear, multiplying the particle's coordinate vector by a matrix can represent the action of any beamline element. This matrix is determined by the properties of the element and is called the transfer matrix for the element. If we represent all the second-order moments of the beam by a symmetric matrix, then the effects of the element on these statistical quantities can be determined by a transpose conjugation with the transfer matrix. This technique is easy to implement on a computer. A transfer matrix can also be used to model the action the beam's space charge if we use a linear fit to the self electric field of the beam. We do this by employing a weighted linear regression, where the weighting factor is the beam distribution. This gives us a fit that is more accurate in regions of higher beam density. It turns out that this field approximation also conforms to the assumption of constant rms emittance, as done in the previous description of the beam dynamics. So we essentially have an equivalent representation as before, only the beam is propagated discretely with transfer matrices.

### 1.2. Outline

In Section 2 we review the basic physics background necessary for this analysis. Mostly this entails placing the common physical concepts in the context of accelerator physics. In particular we cover the design trajectory, phase space, and the equations of motion for an accelerator system. Section 3 introduces the basic statistical concepts on which we rely for our simulation technique. There we show how to transform the equations of motion for individual particles into evolution equations for statistical properties of the beam. Section 4 describes quantities and parameters particular to particle beam physics. The most important of these concepts is probably the rms envelopes and the Courant-Snyder parameters for describing the phase space distribution of the beam. We also cover the mean value vector and the covariance matrix, convenient methods for representing the statistical properties of the beam. Ellipsoidal beams are treated in Section 5, that is, beam distributions having ellipsoidal symmetry. Specifically, we compute the space charge effects for ellipsoidal beams. We see that it is possible to determine the effects of the self-forces analytically in terms of elliptic integrals for distributions having ellipsoidal symmetry in configuration space. Sections 6 and 7 cover simulation techniques for bunched beams with ellipsoidal symmetry. Section 6 treats the envelope equations for bunched beams where we develop the coupled set of ordinary differential equations describing the evolution of the equivalent uniform beam. Section 7 presents the transfer matrix approach to bunched beam envelope simulation. This technique, although somewhat less obvious, is more suited to numerical simulation and is also more general than the envelope equation approach as it can treat coupling between the phase planes. Finally we conclude with Section 8 and present some transfer matrices for common beamline elements in Appendix A.

## 2. PHYSICS BACKGROUND

Here we present the basic physics background for our analysis. Ultimately, we develop the equations of motion for individual beam particles and we do so in a form suitable for beam physics. We also touch upon the various unit conversions and conventions used in the beam physics literature.

### 2.1. The Design Trajectory

We shall assume a beam transport or accelerator system that has a specified design trajectory. This configuration is shown in Figure 1. The distance along this design

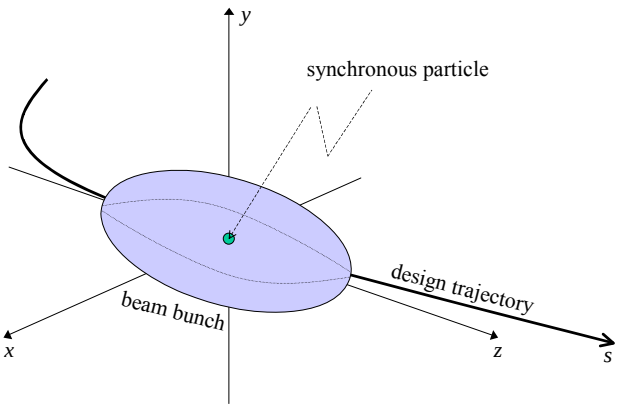


Figure 1: design trajectory and coordinate system

trajectory is given by the independent variable $s$. There also exists the synchronous particle, which has a specified design velocity $v(s)$ at each point $s$ on the design trajectory. The relative velocity $\beta=v/c$ and relativistic parameter $\gamma=1/(1-\beta^2)^{1/2}$ are always given with respect to this design velocity, unless otherwise noted. With respect to the synchronous particle, we construct a system of coordinates $(x,y,z)$, that is, the synchronous particle is at the origin. The coordinates $x,y,z$ represent displacements from the synchronous particle in the $x$, $y$, $z$ directions, respectively. Locally, the $z$-coordinate is always aligned with the design trajectory. Specifically, the tangent vector of the design trajectory always points in the $z$-direction. Thus, the $xy$-plane represents the transverse plane while the $z$-direction is the longitudinal direction of beam propagation (in a local sense). Note that the coordinates $(x,y,z)$ are not the inertial frame of the beam, they are laboratory coordinates that follow the beam.

### 2.2. Phase Space

We form the *phase space* (or *state space*) of the particle by considering the momenta $(x',y',z')$ normalized with respect to the synchronous particle. Let $p(s)=\gamma mv(s)$ represent the mechanical momentum magnitude of the synchronous particle. Then the $x$ and $y$ plane relative momentum $x'$ and $y'$ are given by

$$x' \equiv \frac{dx}{ds} = \frac{p_x}{p} = \frac{\gamma m\dot{x}}{\gamma m\dot{s}}, \qquad y' \equiv \frac{dy}{ds} = \frac{p_y}{p} = \frac{\gamma m\dot{y}}{\gamma m\dot{s}}, \tag{1}$$

where the over dot denotes differentiation with respect to time. For the $z$ plane the situation is different since the coordinate $z$ is defined to be the *difference* in longitudinal position from the synchronous particle, which is traveling at velocity $v$. Therefore,

$$z' \equiv \frac{dz}{ds} = \lim_{\Delta s\to 0}\frac{\Delta z}{\Delta s} = \lim_{\Delta t\to 0}\frac{\Delta t\Delta v}{\Delta tv} = \frac{\Delta v}{v} = \frac{\Delta\beta}{\beta} = \frac{1}{\gamma^2}\frac{\Delta p}{p}, \tag{2}$$

where $\Delta v$ is the difference in velocity $v$ of the synchronous particle, $\Delta\beta$ is the difference in normalized velocity, $\Delta p$ is the difference in longitudinal momentum $p$ of the synchronous particle, and the last equality comes from relativistic mechanics (see below).

The complete set of phase space coordinates for a particle, including both position and normalized momentum, at location $s$ is given by $(x,x',y,y',z,z';s)$. This coordinate space, specifically with the normalized momenta $x'$, $y'$, and $z'$, is also commonly called *trace space* in the literature. For conciseness, it is convenient to denote these points in phase space by a vector quantity, usually $\mathbf{z}$. However, referring to the following section, we reserve $\mathbf{z}$ to denote points in phase space charted with *homogeneous coordinates*.

### 2.3. Homogeneous Coordinates

Points in phase space are represented with the coordinate vector $\mathbf{z}$. It represents the position and momentum of a particle at a particular position $s$ along the beamline. For reasons that become clear later, we work with *homogeneous* phase space coordinates in the space $\Re^6\times\{1\}$. This space is isomorphic to the usual space of phase coordinates $\Re^6$, but contains an additional, constant, coordinate. We have

$$\mathbf{z} \equiv (x, x', y, y', z, z', 1) \in \Re^6 \times \{1\}, \tag{3}$$

where $x,y,z$ are the coordinates in configuration space and the primes indicate differentiation with respect to the path length parameter $s$ (e.g., $y'=dy(s)/ds$).

Homogeneous coordinates are a mathematical technique for parameterizing the projective spaces $P^n$. They are also widely used in computer graphics for three-dimensional rendering, since translation, rotation, and scaling can all be performed by matrix multiplication [20]. The later fact is primary reason that we employ homogeneous coordinates to parameterize phase space (for example, we may represent the action

of a steering dipole magnet as a matrix operation on homogeneous phase space coordinates). Also, the correlation matrix of phase space coordinate moments will contain all moments up to second order, rather than just monomial moments of second order (see Section 4.4).

The remainder of this section constructs the covering of the real projective spaces by homogeneous coordinates; it is not relevant to any material in the sequel. The $n$-dimensional real projective space $\Re P^n$ can be described as a set equivalence relations $[x_0, \ldots, x_n]$ on $\Re^{n+1}$ where $[x_0, \ldots, x_n] \sim [wx_0, \ldots, wx_n]$ for all real $w \neq 0$, and such that not all the $x_i$ are zero. Thus, the points of the project space $\Re P^n$ are seen to be the lines in $\Re^{n+1}$ that pass through the origin. These equivalence classes are known as the homogeneous coordinates of the projective spaces. (Another equivalent description of the projective space $\Re P^n$ is found by identifying all the antipodal points of the sphere $S^n$.)

The projective space $\Re P^n$ can be considered a differentiable manifold with the atlas consisting of $n+1$ charts $\{U_i, \phi_i\}_{i=0}^{n}$ where $U_i$ is the set of equivalence relations $[x_0, \ldots, x_n]$ such that $x_i \neq 0$, and $\phi_i : U_i \to \Re^n$ is the bijective coordinate map

$$\phi_i : [x_0, \ldots, x_i, \ldots x_n] \mapsto (x_0 / x_i, \ldots, \hat{x}_i, \ldots x_n / x_i) . \tag{4}$$

The caret indicates omission of the coordinate. Note that the union $\cup_{i=0}^{n} U_i$ covers all of $\Re P^n$. More aptly, note that the coordinates of the $i=n+1$ chart consist of the following equivalence relations:

$$\phi_i^{-1}(x_0, \ldots, x_{n-1}) = [x_0, \ldots x_{n-1}, 1] \quad \forall (x_0, \ldots x_{n-1}) \in \Re^n . \tag{5}$$

Thus, $U_i$ is seen to be the set of all lines in $\Re^{n+1}$ passing through the plane $\{(x_0, \ldots, x_n) \in \Re^{n+1} \mid x_n = 1\}$. We use the homogeneous coordinates of this chart.

### 2.4. The Longitudinal Phase Plane

Since the $z$ phase plane has several different descriptions in the literature, we shall consider it in more detail. There are several different coordinate systems commonly used to describe this phase plane. Because we are considering position and momentum in the direction of propagation it is necessary to consider relativistic effects when converting between these descriptions. The following equations relate differential changes in common relativistic parameters:

$$\begin{aligned} d\gamma &= \beta\gamma^3 d\beta , \\ d(\beta\gamma) &= \gamma^3 d\beta , \\ dW &= mc^2 d\gamma = \beta\gamma^3 mc^2 d\beta , \end{aligned} \tag{6}$$

where $W$ is the kinetic energy of the particle given by $(\gamma-1)mc^2$.

Commonly used coordinates used in lieu of $z$ are $\Delta\phi$ and $\Delta t$. The coordinate $\Delta\phi$ is the RF phase difference from the synchronous particle, while $\Delta t$ is the difference in arrival time from the synchronous particle. To convert from $\Delta\phi$ in degrees, or $\Delta t$ in seconds, to $z$ in meters use the following formulae:

$$\begin{aligned} z &= vT \frac{-\Delta\phi}{360} = -\beta\lambda \frac{\Delta\phi}{360} , \\ &= -\Delta t(v + \Delta v) = -\beta c \Delta t(1 + z') \approx \beta c \Delta t , \end{aligned} \tag{7}$$

where $T$ is the period of the RF and $\lambda$ is the free-space wavelength of the RF. Note that negative values of $\Delta\phi$ indicate a phase difference ahead of the synchronous particle (a phase lead) while negative values for $\Delta t$ indicate arrival times before the synchronous particle.

Coordinates that alternately describe $z'$ are $\Delta p/p$ and $\Delta W$. The quantity $\Delta p$ is the difference in momentum from the synchronous particle so that $\Delta p/p$ is the normalized difference in momentum. Likewise, $\Delta W$ is the difference in kinetic energy from the synchronous particle. To convert from $\Delta p/p$ in radians or $\Delta W$ in electron volts (Joules) to $z'$ in radians use the relation

$$z' = \frac{1}{\gamma^2}\frac{\Delta p}{p} = \frac{1}{\gamma^2}\frac{\gamma}{(\gamma+1)}\frac{\Delta W}{W}, \tag{8}$$

where $W$ is the beam's kinetic energy, and we have used the fact that

$$\frac{\Delta p}{p} = \frac{\gamma}{\gamma+1}\frac{\Delta W}{W}. \tag{9}$$

These relations follow from the facts that $pc = (E^2 - E_R^2)^{1/2}$, $\Delta p = mc\Delta(\beta\gamma) = \gamma^3 mc\Delta\beta = p\gamma^2(\Delta\beta/\beta)$ and $\Delta W = mc^2\Delta\gamma = \beta^2\gamma mc^2(\Delta p/p)$, where $E = \gamma mc^2$ is the total energy and $E_R = mc^2$ is the rest energy.

### 2.5. Equations of Motion

Newton's second law gives the equations of motion for individual particles of the beam. We shall make all our calculations in the laboratory frame. Recall that the coordinates $(x,y,z)$ are actually the displacements from the synchronous particle on the design trajectory. In our case the familiar $\mathbf{F}=d\mathbf{p}/dt$ appears as

$$\begin{aligned}\mathbf{F} &= \frac{d(\gamma m\mathbf{v})}{dt} = \beta c\frac{d}{ds}(\gamma m\mathbf{v}) \\ &= \beta^2\gamma mc^2\mathbf{r}'' + \beta^2 mc^2(x', y', z'+1)\frac{d\gamma}{ds}\end{aligned} \tag{10}$$

where $\mathbf{F}$ is the force on a particle, $\gamma$ is the relativistic factor, $m$ is the particle mass, $c$ is the speed of light, $\beta \equiv v/c$ where $v$ is velocity of the synchronous particle along $s$, $\mathbf{r}\equiv(x,y,s+z)$ is the position vector, and the primes indicate differentiation with respect to $s$. To derive the second line of the above note that the velocity vector can be expressed as $\mathbf{v}=\beta c(x',y',z'+1)$. The second term of that equation is nonzero only when particles are accelerated. Many times we can assume that the quantity $\gamma'$ is negligible, for example in transport systems or between RF gaps.

The Lorentz force law containing all the electromagnetic fields gives the forces $\mathbf{F}$ on a beam particle. We decompose the force vector $\mathbf{F}$ into the superposition of the applied external forces $\mathbf{F_a}$ and the self-forces $\mathbf{F_s}$ caused by the electromagnetic fields of the beam itself. The applied forces are assumed to be linear by design, since it is known that nonlinear forces can degrade beam quality. Thus,

$$\mathbf{F_a} = -\mathbf{K}(s)\cdot\mathbf{r}, \tag{11}$$

where $\mathbf{K}\equiv(\kappa_x(s),\kappa_y(s),\kappa_z(s))$ represents the action of external beamline components. For example, the focusing force in the $x$-direction applied by a magnetic quadrupole lens is given by

$$F_{a,x} = -q\beta c\frac{\partial B_y(0)}{\partial x}x, \tag{12}$$

where $B_y$ is the $y$-directed magnetic field. Thus, $\kappa_x = q\beta c[\partial B_y/\partial x]$.

The self-forces $\mathbf{F_s}$ are the electromagnetic fields produced by the beam itself. We have

$$\mathbf{F_s} = q\mathbf{E_s}(\mathbf{r},s) + q\beta c[\mathbf{r}' + \mathbf{a_z}]\times\mathbf{B_s}(\mathbf{r},s), \tag{13}$$

where $\mathbf{E_s}$ is the self electric field, $\mathbf{B_s}$ is the self magnetic field, and $\mathbf{a_z}$ is the unit vector in the direction of the design trajectory (i.e., it points in the $z$-direction). The individual velocities around the synchronous particle, given by $\mathbf{r}'$, is typically negligible compared to the collective motion of the bunch. Consequently we drop the $\mathbf{r}'$. This action leads to magnetic self-fields that are directly proportional to the electric self-fields in the perpendicular direction. The reason for this situation is that the collective motion along the design trajectory produces the magnetic fields. (Forces from longitudinal magnetic fields will be zero by the cross product.) We have

$$\mathbf{B}_\perp = \frac{\beta}{c}\mathbf{a_z}\times\mathbf{E_s}, \tag{14}$$

where $\mathbf{B}_\perp$ is the magnetic field perpendicular to $\mathbf{a}_z$. Consequently, the perpendicular force has the form $\mathbf{F}_\perp=(1-\beta^2)\mathbf{E}_\perp$, where $\mathbf{E}_\perp$ is the perpendicular self electric field. The parallel self-force depends only on the parallel self electric field. Collecting these results, the forces in all three directions can be written

$$
\begin{aligned}
F_x &= -\kappa_x(s)x + \frac{q}{\gamma^2}E_x(x,y,z;s),\\
F_y &= -\kappa_y(s)y + \frac{q}{\gamma^2}E_y(x,y,z;s),\\
F_z &= -\kappa_z(s)z + qE_z(x,y,z;s).
\end{aligned}
\tag{15}
$$

The resulting equations of motion for a beam particle are

$$
\begin{aligned}
x'' + \frac{\gamma'}{\gamma}x' + \frac{\kappa_x}{\gamma mc^2\beta^2}x &= \frac{q}{\gamma^3 mc^2\beta^2}E_x,\\
y'' + \frac{\gamma'}{\gamma}y' + \frac{\kappa_y}{\gamma mc^2\beta^2}y &= \frac{q}{\gamma^3 mc^2\beta^2}E_y,\\
z'' + \frac{\gamma'}{\gamma}z' + \frac{\kappa_z}{\gamma mc^2\beta^2}z &= -\frac{\gamma'}{\gamma} + \frac{q}{\gamma mc^2\beta^2}E_z.
\end{aligned}
\tag{16}
$$

Now we simplify the equations with some standard definitions. First, let

$$
k_\alpha^2 \equiv \frac{\kappa_\alpha}{\gamma mc^2\beta^2} \quad \text{where} \quad \alpha \in \{x,y,z\},
\tag{17}
$$

which are the linear proportionality constants for the external focusing. We further reduce the above equation set by introducing a standard parameter in beam physics, the *beam perveance K*. This is a measure of the space-charge effect and we define it as

$$
K \equiv \frac{qN}{2\pi\varepsilon_0}\frac{1}{\gamma^3\beta^2}\frac{q}{mc^2} = \frac{qN}{2\pi\varepsilon_0}\frac{1}{\gamma^3\beta^2}\frac{1}{E_R},
\tag{18}
$$

where $\varepsilon_0$ is the permittivity of free space, $N$ is the total number of particles in the beam bunch, and $E_R = q/mc^2$ is the rest energy of the bunch particles in electron-Volts. This definition is somewhat different than that of other authors [24][25]; it is more useful for the present discussion. Unfortunately, there is no standard definition for the bunched beam perveance, as there is for continuous beams. But we can reconcile this definition with that for a continuous beam by considering the charge $Q$ of a beam. For our bunched beam this value is easily recognized as $Q = qN$. It can also be expressed in terms of the beam current $I$ as

$$
Q = I / f,
\tag{19}
$$

where $f$ is the drive frequency of the RF cavity. For a continuous beam we can define $Q$ by the relation $I = vQ$ where $v$ is the beam velocity and $Q$ is now the charge per unit length of the beam. Substituting $Q = I/v$ into the equation for $K$ yields

$$
K \equiv \frac{I}{2\pi\varepsilon_0}\frac{1}{\gamma^3\beta^3}\frac{q}{mc^3},
\tag{20}
$$

which is the expression typically seen in the literature.

With these definitions the resulting equations of motion are

$$
\begin{aligned}
&x'' + \frac{\gamma'}{\gamma} x' + k_x^2 x = K \frac{2\pi\varepsilon_0}{Q} E_x \,, \\
&y'' + \frac{\gamma'}{\gamma} y' + k_y^2 y = K \frac{2\pi\varepsilon_0}{Q} E_y \,, \\
&z'' + \frac{\gamma'}{\gamma} z' + k_z^2 z = -\frac{\gamma'}{\gamma} + \gamma^2 K \frac{2\pi\varepsilon_0}{Q} E_z \,.
\end{aligned} \tag{21}
$$

## 3. STATISTICS BACKGROUND

### 3.1. The Density Function

Assume that the particle beam can be described by a density distribution function *f* of the particles' phase space coordinates (*x, x', y, y', z, z'*)~(*x, x', y, y', z, z',*1) and position along the design trajectory *s*. That is, the entire ensemble of beam particles is represented by the function *f*. The function *f* describes the distribution of the beam's mass (or charge) in phase space at each location *s* along the beamline. It can also be interpreted as a probably density function characterizing the probability that any particle occupies a particular region of phase space at location *s*. Thus, the probably that a particle lies in the infinitesimal phase space volume *dxdx'dydy'dzdz'* centered at (*x, x', y, y', z, z'*) and located at position *s* along the beamline is

$$f(x, x', y, y', z, z'; s) dx dx' dy dy' dz dz' \,. \tag{22}$$

Typically we assume that the particle ensemble is populous enough to be represented accurately by a continuous *f*. However, it is always possible to formulate a discrete ensemble by assuming that *f* is a summation of displaced Dirac delta functions. Finally, note that the function *f*(*x,x',y,y',z,z';s*) contains all the information of the beam but requires an enormous amount of storage space to represent on a computer, it is a function of seven independent variables.

The evolution of the function *f* is governed by the Vlasov equation, which incorporates the equations of motion and the Lorentz force equation. It is a partial differential equation containing partial derivatives of all seven independent variables and is typically intractable to solve in general. We shall avoid the Vlasov equation by propagating only a small subset of the distribution's *moments*. For this we require only the equations of motion and Liouville's theorem.

### 3.2. Liouville's Theorem

Liouville's theorem states that the total derivate of *f* with respect to *s* along particle trajectories is zero, or formally

$$\frac{d}{ds} f[x(s), x'(s), y(s), y'(s), z(s), z'(s); s] = 0 \,. \tag{23}$$

Note that this is a convective derivative that follows the particle trajectory. The fully expanded derivative is

$$\frac{\partial f}{\partial x} x' + \frac{\partial f}{\partial x'} x'' + \frac{\partial f}{\partial y} y' + \frac{\partial f}{\partial y'} y'' + \frac{\partial f}{\partial z} z' + \frac{\partial f}{\partial z'} z'' + \frac{\partial f}{\partial s} = 0 \,, \tag{24}$$

where *x''=dx'/ds*, etc.

This is essentially a statement of the conservation of mass. The practical considerations where the theorem holds true are for collisionless systems where there are ample enough particles such that the self-fields are represented accurately by smooth functions. That is, there is no "graininess" of individual particles; the distribution behaves much like a fluid. Otherwise, Liouville's theorem is true only for distribution functions on 6*N* dimensional phase space, where *N* is the number of particles.

We mention in passing that by substituting the Lorentz force laws for $x''$, $y''$, and $z''$ in the above we obtain the Vlasov equation. Thus, the trajectories $\{\mathbf{z}(s)\}$ where the above holds actually represent the characteristic lines of the Vlasov equation.

### 3.3. Moments of the Distribution

Moments of the distribution are function averages on phase space, weighted with respect to the distribution function. For example, let $g(x, x', y, y', z, z')$ be some arbitrary function on phase space, then the moment of $g$, denoted $\langle g \rangle$, is given by

$$\begin{aligned} \langle g \rangle &\equiv \frac{1}{N} \int g(x,x',y,y',z,z') f(x,x',y,y',z,z';s)\, dx dx' dy dy' dz dz', \\ &= \frac{1}{N} \int g(\mathbf{z}) f(\mathbf{z})\, d^6\mathbf{z}, \end{aligned} \tag{25}$$

where the integration is taken over all of phase space,

$$d^6\mathbf{z} \equiv dx dx' dy dy' dz dz', \tag{26}$$

is the single basis on phase space 6-forms, and

$$N \equiv \int f(\mathbf{z};s)\, d^6\mathbf{z}, \tag{27}$$

is the total number of particles in the ensemble. (In mathematical parlance, we can view $f$ as a measure on phase space.) Note that with this definition $\langle g \rangle$ is still a function of $s$ because $f$ is a function of $s$. We shall be concerned foremost with the moments of phase space monomials, that is, moments of the form $\langle x \rangle$, $\langle x' \rangle$, $\langle x^2 \rangle$, $\langle xx' \rangle$, $\langle x'^2 \rangle$ and their counterparts for the other phase space coordinates. Theses moments represent the evolution of the beam's statistics, in particular the center of mass (average position and velocity) and the rms envelopes of the beam.

Notice also that in the above definition $\langle \cdot \rangle$ is normalized. It is normalized by the total number of particles, a factor $1/N$, so that the moment of 1 is 1, that is $\langle 1 \rangle = 1$.

### 3.4. Moment Equations

Liouville's theorem enables us to formulate evolution equations for the moments of the beam. Specifically it allows the moment operator $\langle \cdot \rangle$ and the differentiation operator $d\cdot/ds$ to commute. For example, if $g(\mathbf{z};s)$ is a function of the phase space coordinates and $s$, then the derivative of $\langle g \rangle$ with respect to $s$ is given as

$$\begin{aligned} \langle g \rangle' &\equiv \frac{d}{ds}\langle g \rangle = \frac{d}{ds}\frac{1}{N}\int g(\mathbf{z};s) f(\mathbf{z};s)\, d^6\mathbf{z} = \frac{1}{N}\int \left[ g'(\mathbf{z};s) f(\mathbf{z};s) + g(\mathbf{z};s) f'(\mathbf{z};s) \right] d^6\mathbf{z}, \\ &= \langle g' \rangle \end{aligned} \tag{28}$$

Thus, we are able to move differentiation with respect to $s$ within the moment operator and vice-versa.

Now we may average the equations of motion with respect to the beam ensemble then employ Liouville's theorem to commute the differentiations with respect to $s$. In the $x$-plane, we have for the first moments

$$\begin{aligned} \langle x \rangle' &= \langle x' \rangle, \\ \langle x' \rangle' &= \langle x'' \rangle = -k_x^2 \langle x \rangle - \frac{\gamma'}{\gamma}\langle x' \rangle + K \frac{2\pi\varepsilon_0}{qN}\langle E_x \rangle. \end{aligned} \tag{29}$$

The quantity $\langle E_x \rangle$ is zero for *symmetric* charge distributions by pair-wise cancellation. Since we assume that the beam has an ellipsoidally symmetric charge distribution in the sequel, we neglect this term. We then have the following equations for the first-order moments:

$$
\begin{aligned}
&\langle x\rangle' = \langle x'\rangle, && \langle y\rangle' = \langle y'\rangle, && \langle z\rangle' = \langle z'\rangle,\\
&\langle x'\rangle' = -k_x^2\langle x\rangle - \frac{\gamma'}{\gamma}\langle x'\rangle && \langle y'\rangle' = -k_y^2\langle y\rangle - \frac{\gamma'}{\gamma}\langle y'\rangle && \langle z'\rangle' = -k_z^2\langle z\rangle - \frac{\gamma'}{\gamma}\left[\langle z'\rangle + 1\right]
\end{aligned} \tag{30}
$$

Notice that the above equations are independent of the self-fields and represent the equations of motion for the beam's center of mass; they form a complete set. Thus, these equations may be propagated independently. To simplify the analysis in what follows, we often assume a centered beam to make computations easier. We can then displace this centered beam according to the above equations describing the centroid motion.

Now consider the second-order moments of the form $\langle x^2\rangle$, $\langle xx'\rangle$, $\langle x'^2\rangle$. Proceeding as before, the equations for the $x$-plane moments are

$$
\begin{aligned}
&\langle x^2\rangle' = \langle (x^2)'\rangle = 2\langle xx'\rangle\\
&\langle xx'\rangle' = \langle x'^2\rangle + \langle xx''\rangle = \langle x'^2\rangle - \frac{\gamma'}{\gamma}\langle xx'\rangle - k_x^2\langle x^2\rangle + K\frac{2\pi\varepsilon_0}{qN}\langle xE_x\rangle\\
&\langle x'^2\rangle' = 2\langle x'x''\rangle = -2k_x^2\langle xx'\rangle - 2\frac{\gamma'}{\gamma}\langle x'^2\rangle + 2K\frac{2\pi\varepsilon_0}{qN}\langle x'E_x\rangle
\end{aligned} \tag{31}
$$

There exist similar equations for the $y$ moments. The $z$ second moment equations are

$$
\begin{aligned}
&\langle z^2\rangle' = 2\langle zz'\rangle\\
&\langle zz'\rangle' = \langle z'^2\rangle - \frac{\gamma'}{\gamma}\langle zz'\rangle - k_z^2\langle z^2\rangle - \frac{\gamma'}{\gamma}\langle z\rangle + \gamma^2 K\frac{2\pi\varepsilon_0}{qN}\langle zE_z\rangle\\
&\langle z'^2\rangle' = -2k_z^2\langle zz'\rangle - 2\frac{\gamma'}{\gamma}\langle z'^2\rangle - 2\frac{\gamma'}{\gamma}\langle z'\rangle + 2\gamma^2 K\frac{2\pi\varepsilon_0}{qN}\langle z'E_z\rangle
\end{aligned} \tag{32}
$$

In general we may also have cross moments of the form $\langle xy\rangle$, $\langle x'y\rangle$, $\langle xy'\rangle$, and $\langle x'y'\rangle$. The cross moments would typically result from bending magnets or misaligned beamline elements.

From this point two differing approaches to simulation are typically employed: 1) we use the second-order moment equations to develop a set of ordinary differential equations describing the rms envelopes of the beam, this technique is covered in Section 6. 2) We propagate the entire set of second-order moments in the form of a symmetric correlation matrix, this technique is covered in Section 7. The later approach is more general than the former, since it can treat rotated ellipsoids and external coupling between phase planes.

## 4. BEAM PHYSICS

In this section we outline quantities and concepts that are particular to beam physics. Specifically, we cover rms envelopes, rms emittance, and the rms phase space ellipse. We also consider a linear approximation to the self-fields that is particularly important for beam physics calculations.

### 4.1. The RMS Envelopes

Here we introduce the notion of rms beam envelopes, which is fundamental in much of the beam physics literature. The rms envelopes of a beam represent the boundary of the beam in a collective, or statistical sense. As we see in the sequel, for ellipsoidally symmetric beams this statistical behavior is almost independent of the actual profile of the beam distribution. That is, the rms envelopes of many beams behave the same regardless of the actual distribution.

First, let us consider the mean values of the particle distribution. We use $\bar{x}, \bar{y}, \bar{z}$ to denote theses first-order spatial moments, that is

$$\bar{x} = \langle x \rangle, \qquad \bar{y} = \langle y \rangle, \qquad \bar{z} = \langle z \rangle . \tag{33}$$

These values are the positions of the center of mass in the *x*, *y*, and *z* directions, respectively. That is, they are the coordinates of the beam centroid.

Now we consider the rms envelopes of the beam. To do so we first introduce the following definitions:

$$\begin{aligned} \tilde{x} &\equiv \langle x^2 \rangle^{1/2}, \\ \tilde{y} &\equiv \langle y^2 \rangle^{1/2}, \\ \tilde{z} &\equiv \langle z^2 \rangle^{1/2}. \end{aligned} \tag{34}$$

In the literature these quantities are commonly referred to as the rms envelopes of the beam. It is important to point out that this is only true for a centered beam. The *true* rms envelopes of a beam are actually the standard deviations of the density distribution *f*. Denoting the standard deviations in the *x*, *y*, and *z* directions as $\sigma_x$, $\sigma_y$, $\sigma_z$, respectively, they are defined

$$\begin{aligned} \sigma_x &\equiv \langle (x-\bar{x})^2 \rangle^{1/2} = \left[ \langle x^2 \rangle - \bar{x}^2 \right]^{1/2}, \\ \sigma_y &\equiv \langle (y-\bar{y})^2 \rangle^{1/2} = \left[ \langle y^2 \rangle - \bar{y}^2 \right]^{1/2}, \\ \sigma_z &\equiv \langle (z-\bar{z})^2 \rangle^{1/2} = \left[ \langle z^2 \rangle - \bar{z}^2 \right]^{1/2}, \end{aligned} \tag{35}$$

or

$$\sigma_x = \left[ \tilde{x}^2 - \bar{x}^2 \right]^{1/2}, \quad \sigma_y = \left[ \tilde{y}^2 - \bar{y}^2 \right]^{1/2}, \quad \sigma_z = \left[ \tilde{z}^2 - \bar{z}^2 \right]^{1/2} . \tag{36}$$

Note that when the beam is centered, that is when $\bar{x} = \bar{y} = \bar{z} = 0$, the rms envelopes $\sigma_x$, $\sigma_y$, $\sigma_z$ are equal to the quantities $\tilde{x}, \tilde{y}, \tilde{z}$. This is the situation most often encountered in the literature. Typically a centered beam is assumed to simplify computations, particularly for the moments $\langle xE_x \rangle$, $\langle yE_y \rangle$, and $\langle zE_z \rangle$. A common approximation in simulation is the assumption that the beam is centered when computing the evolution of the second moments $\tilde{x}, \tilde{y}, \tilde{z}$; the offsets $\bar{x}, \bar{y}, \bar{z}$ are computed independently to form the complete beam state.

### 4.2. RMS Emittance

One particularly important quantity in beam physics is the rms emittance, usually denoted $\tilde{\varepsilon}$. This is a figure of merit indicating the area in each phase plane that the rms beam envelope occupies. The rms emittance is a function of the second moments, for each phase plane it is defined

$$\begin{aligned} \tilde{\varepsilon}_x &\equiv \left[ \langle x^2 \rangle \langle x'^2 \rangle - \langle xx' \rangle^2 \right]^{1/2}, \\ \tilde{\varepsilon}_y &\equiv \left[ \langle y^2 \rangle \langle y'^2 \rangle - \langle yy' \rangle^2 \right]^{1/2}, \\ \tilde{\varepsilon}_z &\equiv \left[ \langle z^2 \rangle \langle z'^2 \rangle - \langle zz' \rangle^2 \right]^{1/2}. \end{aligned} \tag{37}$$

It is known that whenever all forces acting on the beam are linear and there is no acceleration, the rms emittance is an invariant of the motion [9][12][14]. An increasing emittance is usually indicative of a loss in beam quality. Thus, the rms emittance of a beam typically increases whenever unwanted nonlinear forces are encountered.

When the beam is accelerated the transverse rms emittances always decrease. This condition is simply an artifact of the definitions of *x′* and *y′* and does not imply any decrease in random transverse kinetic

energy (temperature). Since $x'=p_x/p$, it decreases with increasing longitudinal momentum $p$, which in turn decreases the rms emittance. To see this consider the $x$ phase plane and assume that the self-fields can be represented as the linear function $E_x=ax$, where $a$ is a real number. Now simply differentiate the definition of rms emittance

$$\begin{aligned}\frac{d}{ds}\tilde{\varepsilon}_x^2 &= \left\langle x^2\right\rangle'\left\langle x'^2\right\rangle + \left\langle x^2\right\rangle\left\langle x'^2\right\rangle' - 2\left\langle xx'\right\rangle\left\langle xx'\right\rangle', \\ &= -2\frac{\gamma'}{\gamma}\tilde{\varepsilon}_x^2 ,\end{aligned} \tag{38}$$

where the second line is obtained by substituting the derivatives from Eqs. (31). The solution to this equation is

$$\tilde{\varepsilon}_x^2(s) = \frac{\tilde{\varepsilon}_{x,0}^2}{\gamma^2(s)}, \tag{39}$$

where $\tilde{\varepsilon}_{x,0}$ is the initial value. Thus, we can see outright that when the beam energy increases the transverse rms emittances decrease. Applying the same procedures to the longitudinal plane we get a different equation

$$\frac{d}{ds}\tilde{\varepsilon}_z^2 = -2\frac{\gamma'}{\gamma}\tilde{\varepsilon}_z^2 + 2\frac{\gamma'}{\gamma}\left\langle z\right\rangle\left\langle zz'\right\rangle . \tag{40}$$

Thus, if the RF phase is misaligned during acceleration, causing a nonzero $\langle z\rangle$, it is actually possible to experience emittance growth in the longitudinal plane.

To alleviate the situation of decreasing transverse emittances with acceleration we may alternately use the *normalized rms emittances*, typically denoted $\tilde{\varepsilon}_n$. These emittances are defined as [24]

$$\tilde{\varepsilon}_{n,x} \equiv \beta\gamma\tilde{\varepsilon}_x , \qquad \tilde{\varepsilon}_{n,y} \equiv \beta\gamma\tilde{\varepsilon}_y , \qquad \tilde{\varepsilon}_{n,z} \equiv \beta\gamma\tilde{\varepsilon}_z . \tag{41}$$

Performing a similar analysis as with the rms emittances using similar assumptions, we find that the normalized rms transverse emittances behave as

$$\tilde{\varepsilon}_{n,x}(s) = \beta(s)\,\tilde{\varepsilon}_{n,x,0}, \tag{42}$$

where $\tilde{\varepsilon}_{n,x,0}$ is an arbitrary constant. Thus, the transverse normalized rms emittances actually increase with increasing beam energy. However, once the beam velocity approaches $c$ these emittances level off with increasing beam energy.

In our phase space coordinates the units of rms emittance are meter-radians. However, recalling that there are several alternate coordinate systems for the $z$ phase plane, it is common to find emittance values for this plane given in several different units. When the $z$ phase plane coordinates are $(z,\Delta p/p)$ the units are meter-radians. When the coordinates are $(\Delta\phi,\Delta W)$ the units are degrees-electron volts. Finally, when the coordinates are $(\Delta t, \Delta W)$ the units are seconds-electron volts. To convert between theses units to meter-radians we substitute the coordinate conversion formulas (7) and **Error! Reference source not found.** into the above definition for $\tilde{\varepsilon}_z$. The results are

$$\begin{aligned}\tilde{\varepsilon}_z\ (\mathrm{m-rad}) &= C_{\Delta p}\,\tilde{\varepsilon}_z\ (\mathrm{m\text{-}rad}), \\ &= C_{\mathrm{deg}}\,\tilde{\varepsilon}_z\ (\mathrm{deg-eV}), \\ &= C_{\mathrm{sec}}\,\tilde{\varepsilon}_z\ (\mathrm{sec-eV}),\end{aligned} \tag{43}$$

where the conversion factors $C_{\Delta p}$, $C_{\mathrm{deg}}$ and $C_{\mathrm{sec}}$ are defined

$$C_{\Delta p} \equiv \frac{1}{\gamma^2} \text{ (no units)},$$

$$C_{\deg} \equiv \frac{\beta\lambda}{360}\frac{1}{\gamma^2}\frac{\gamma}{(\gamma+1)}\frac{1}{W} = \frac{\lambda}{360}\frac{1}{\gamma^2}\frac{1}{p_0 c} \left(\frac{\text{m}-\text{rad}}{\text{deg}-\text{eV}}\right), \tag{44}$$

$$C_{\sec} \equiv \frac{\beta c}{\gamma^2}\frac{\gamma}{\gamma+1}\frac{1}{W} = \frac{1}{\gamma^2}\frac{1}{p_0} \left(\frac{\text{m}-\text{rad}}{\text{sec}-\text{eV}}\right),$$

where $E_R = mc^2/q$ is the rest energy of the beam particles in electron volts, and $p_0 = \beta_0\gamma_0 mc$ is the momentum of the synchronous particle ($p_0 c$ in $eV$). Note that the beam energy $W$ must also be given in electron-volts.

### 4.3. Courant-Snyder Parameters for the RMS Ellipse

When modeling beam distributions, the projections of the distributions onto each phase plane are represented ideally by an ellipse. Here we introduce the Courant-Snyder, or Twiss, parameters often found in the literature. These parameters describe the projections of the beam distribution onto the phase space planes. In particular, we shall describe the ellipse relating to the second-order moments of the beam (the rms moments). This ellipse is congruent to the phase space ellipse of the equivalent uniform beam. To make explicit calculations we consider the $x$ phase plane with the coordinates ($x$,$x'$). There are analogous results for the $y$ and $z$ phase planes.

Consider an ellipse centered in $x$ phase space as shown in Figure 2. The general equation for such an ellipse can be expressed

$$\gamma_x x^2 + 2\alpha_x x x' + \beta_x x'^2 = \tilde{\varepsilon}_x, \tag{45}$$

where $\alpha_x$, $\beta_x$, $\gamma_x$ are known as the Courant-Snyder parameters for the $x$ phase plane. These parameters are not independent; they are related through the equation

$$\beta_x\gamma_x - \alpha_x^{\,2} = 1. \tag{46}$$

This relation enforces the area enclosed by the ellipse to be $\pi\tilde{\varepsilon}_x$, otherwise, the area would be $\pi\tilde{\varepsilon}_x/(\beta_x\gamma_x - \alpha_x^2)$. Note that Eq. (45) can be written in the matrix vector format

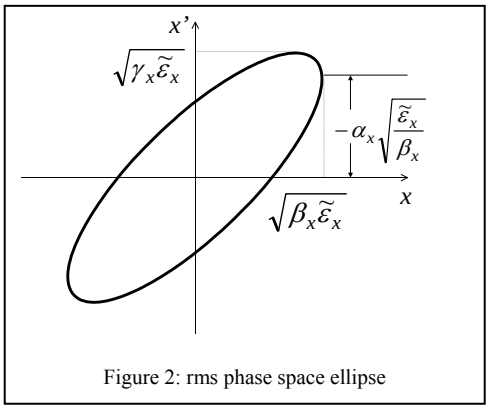

Figure 2: rms phase space ellipse

$$\begin{pmatrix} x \\ x' \end{pmatrix}^T \begin{pmatrix} \gamma_x & \alpha_x \\ \alpha_x & \beta_x \end{pmatrix} \begin{pmatrix} x \\ x' \end{pmatrix} = \tilde{\varepsilon}_x, \tag{47}$$

where the determinant of the above matrix is unity by Eq. (46). Thus, the Twiss parameters are

It is our desire to relate this ellipse to the rms quantities of the beam distribution.

We can solve Eq. (45) for the particular values of $x$ and $x'$ in the phase space shown in Figure 2 (for example, see [24] and [25]). Consider the projections of this ellipse onto the $x$ and $x'$ axes. We want the maximum extent of these projections to be equal to the rms quantities for $x$ and $x'$, respectively. This condition leads to the definitions

$$\sqrt{\beta_x\tilde{\varepsilon}_x} \equiv \left\langle x^2 \right\rangle^{1/2},$$

$$\alpha_x\tilde{\varepsilon}_x \equiv -\left\langle x x' \right\rangle, \tag{48}$$

$$\sqrt{\gamma_x\tilde{\varepsilon}_x} \equiv \left\langle x'^2 \right\rangle^{1/2},$$

where the second equation follows from Eq. (46) and the definition of rms emittance (37).

If the coordinates for the longitudinal phase plane are given as ($\Delta\phi$,$\Delta W$), the conversion of the Courant-Snyder parameters to the ($z$,$z'$) units is given by the following:

$$\begin{aligned}
&\alpha_z\ (\text{no units}) = -\alpha_z\ (\text{no units}),\\
&\beta_z\,(\text{m/rad}) = \frac{\beta\lambda}{360}\frac{\gamma^2}{1}\frac{(\gamma+1)}{\gamma}\frac{W}{1}\ \beta_z\ (\text{deg/eV}),\\
&\gamma_z\,(\text{rad/m}) = \frac{360}{\beta\lambda}\frac{1}{\gamma^2}\frac{\gamma}{(\gamma+1)}\frac{1}{W}\ \gamma_z\ (\text{eV/deg}),
\end{aligned} \tag{49}$$

where, due to an unfortunate choice of notation, we have $\beta$'s and $\gamma$'s representing both relativistic parameters and Courant-Snyder parameters. The grouping of terms was chosen to make the context clear. When the longitudinal coordinates are given as ($z$,$\Delta p/p$), the conversion of the Courant-Snyder parameters to ($z$,$z'$) units is

$$\begin{aligned}
&\alpha_z\ (\text{no units}) = \alpha_z\ (\text{no units}),\\
&\beta_z\,(\text{m/rad}) = \gamma^2\ \beta_z\ (\text{m/rad}),\\
&\gamma_z\,(\text{rad/m}) = \frac{1}{\gamma^2}\ \gamma_z\ (\text{rad/m}),
\end{aligned} \tag{50}$$

When the longitudinal coordinates are given as ($\Delta t$,$\Delta W$), the conversion of the Courant-Snyder parameters to the ($z$,$z'$) units is given by

$$\begin{aligned}
&\alpha_z\ (\text{no units}) = -\alpha_z\ (\text{no units}),\\
&\beta_z\,(\text{m/rad}) = \beta c\frac{\gamma^2}{1}\frac{\gamma+1}{\gamma}\frac{W}{1}\beta_z\ (\text{sec/eV}),\\
&\gamma_z\,(\text{rad/m}) = \frac{1}{\beta c}\frac{1}{\gamma^2}\frac{\gamma}{\gamma+1}\frac{1}{W}\gamma_z\ (\text{sec}-\text{deg}).
\end{aligned} \tag{51}$$

### 4.4. The Mean Value Vector and Correlation Matrix

Here we introduce the mean-value vector $\bar{\mathbf{z}}$ and symmetric 7×7 correlation matrix $\boldsymbol{\chi}$. These quantities contain the state of the beam statistics up to second order. Maintaining consistency with previous notation, let the moments $\langle x'\rangle$, $\langle y'\rangle$, and $\langle z'\rangle$ be denoted

$$\bar{x}' \equiv \langle x' \rangle \qquad \bar{y}' \equiv \langle y' \rangle \quad \text{and} \quad \bar{z}' \equiv \langle z' \rangle, \tag{52}$$

respectively. We accordingly denote the vector of first-order moments as

$$\begin{aligned}
\bar{\mathbf{z}} &\equiv \langle \mathbf{z} \rangle\\
&= \left(\langle x\rangle \quad \langle x'\rangle \quad \langle y\rangle \quad \langle y'\rangle \quad \langle z\rangle \quad \langle z'\rangle \quad 1\right)^T,\\
&= \left(\bar{x} \quad \bar{x}' \quad \bar{y} \quad \bar{y}' \quad \bar{z} \quad \bar{z}'\right)^T,
\end{aligned} \tag{53}$$

where the superscript $T$ indicates transposition. Thus, $\bar{\mathbf{z}}$ is the column vector of mean values for the phase space coordinates. Note that $\bar{\mathbf{z}}$ can be a function of the path length parameter $s$.

When considering the set of second-order moments of the beam it is convenient to work with a matrix whose elements are these moments. We can form such a matrix by taking the moment of the outer product $\mathbf{z}\mathbf{z}^T$. Denote the result as $\boldsymbol{\chi}$ we have

$$(54)\qquad \boldsymbol{\chi} \equiv \left\langle \mathbf{z}\mathbf{z}^T \right\rangle = \begin{pmatrix} \langle x^2 \rangle & \langle xx' \rangle & \langle xy \rangle & \langle xy' \rangle & \langle xz \rangle & \langle xz' \rangle & \langle x \rangle \\ \langle xx' \rangle & \langle x'^2 \rangle & \langle x'y \rangle & \langle x'y' \rangle & \langle x'z \rangle & \langle x'z' \rangle & \langle x' \rangle \\ \langle xy \rangle & \langle x'y \rangle & \langle y^2 \rangle & \langle yy' \rangle & \langle yz \rangle & \langle yz' \rangle & \langle y \rangle \\ \langle xy' \rangle & \langle x'y' \rangle & \langle yy' \rangle & \langle y'^2 \rangle & \langle y'z \rangle & \langle y'z' \rangle & \langle y' \rangle \\ \langle xz \rangle & \langle x'z \rangle & \langle yz \rangle & \langle y'z \rangle & \langle z^2 \rangle & \langle zz' \rangle & \langle z \rangle \\ \langle xz' \rangle & \langle x'z' \rangle & \langle yz' \rangle & \langle y'z' \rangle & \langle zz' \rangle & \langle z'z' \rangle & \langle z' \rangle \\ \langle x \rangle & \langle x' \rangle & \langle y \rangle & \langle y' \rangle & \langle z \rangle & \langle zz' \rangle & 1 \end{pmatrix}.$$

The matrix $\boldsymbol{\chi}$ is called the *correlation matrix* of the beam distribution. The matrix $\boldsymbol{\chi}$ represent all the moments up to, and including, order two at each position $s$ along the beam line. Thus, $\boldsymbol{\chi}$ contains the complete description of the beam's statistical behavior up to order two. This is a convenient representation for the beam state when doing simulation. Because of its statistical nature, $\boldsymbol{\chi}$ is a symmetric, positive semi-definite matrix. Thus, it always has a complete set of eigenvalues and orthonormal eigenvectors.

It is sometimes convenient to decompose $\boldsymbol{\chi}$ into sub-matrices corresponding to the individual phase planes. For example, considering each phase plane $x$, $y$, $z$ whose coordinates are represented by the respective vectors

$$(55)\qquad \begin{aligned} \mathbf{x}(s) &\equiv \begin{pmatrix} x(s) & x'(s) \end{pmatrix}^T, \\ \mathbf{y}(s) &\equiv \begin{pmatrix} y(s) & y'(s) \end{pmatrix}^T, \\ \boldsymbol{\zeta}(s) &\equiv \begin{pmatrix} z(s) & z'(s) \end{pmatrix}^T. \end{aligned}$$

then the sub-matrices for the $x$, $y$, and $z$ phase planes are given as $\langle \mathbf{x}\mathbf{x}^T \rangle$, $\langle \mathbf{y}\mathbf{y}^T \rangle$, $\langle \boldsymbol{\zeta}\boldsymbol{\zeta}^T \rangle$. Denoting these sub-matrices as $\boldsymbol{\chi}_{\mathbf{xx}}$, $\boldsymbol{\chi}_{\mathbf{yy}}$, $\boldsymbol{\chi}_{\mathbf{zz}}$, respectively, we have

$$(56)\quad \boldsymbol{\chi}_{\mathbf{xx}} \equiv \left\langle \mathbf{x}\mathbf{x}^T \right\rangle = \begin{pmatrix} \langle x^2 \rangle & \langle xx' \rangle \\ \langle xx' \rangle & \langle x'^2 \rangle \end{pmatrix}, \quad \boldsymbol{\chi}_{\mathbf{yy}} \equiv \left\langle \mathbf{y}\mathbf{y}^T \right\rangle = \begin{pmatrix} \langle y^2 \rangle & \langle yy' \rangle \\ \langle yy' \rangle & \langle y'^2 \rangle \end{pmatrix}, \quad \boldsymbol{\chi}_{\mathbf{zz}} \equiv \left\langle \boldsymbol{\zeta}\boldsymbol{\zeta}^T \right\rangle = \begin{pmatrix} \langle z^2 \rangle & \langle zz' \rangle \\ \langle zz' \rangle & \langle z'^2 \rangle \end{pmatrix},$$

Thus, the matrix $\boldsymbol{\chi}_{\mathbf{xx}}$ is the correlation matrix of the $x$ phase plane, ignoring coupling, likewise for the $y$ and $z$ planes. We have one such 2×2 matrix for each phase plane, plus we have matrices containing the cross-correlations between phase planes such as $\langle \mathbf{x}\mathbf{y}^T \rangle$, $\langle \mathbf{x}\boldsymbol{\zeta}^T \rangle$, and $\langle \mathbf{y}\boldsymbol{\zeta}^T \rangle$. The full second-order moment matrix $\boldsymbol{\chi}$ has the block matrix form

$$(57)\qquad \boldsymbol{\chi} \equiv \left\langle \mathbf{z}\mathbf{z}^T \right\rangle = \begin{pmatrix} \boldsymbol{\chi}_{\mathbf{xx}} & \boldsymbol{\chi}_{\mathbf{xy}} & \boldsymbol{\chi}_{\mathbf{xz}} & \bar{\mathbf{x}} \\ \boldsymbol{\chi}_{\mathbf{yx}} & \boldsymbol{\chi}_{\mathbf{yy}} & \boldsymbol{\chi}_{\mathbf{yz}} & \bar{\mathbf{y}} \\ \boldsymbol{\chi}_{\mathbf{zx}} & \boldsymbol{\chi}_{\mathbf{zy}} & \boldsymbol{\chi}_{\mathbf{zz}} & \bar{\mathbf{z}} \\ \bar{\mathbf{x}}^T & \bar{\mathbf{y}}^T & \bar{\mathbf{z}}^T & 1 \end{pmatrix},$$

where each $\boldsymbol{\chi}_{\alpha\beta}$ is a 2×2 symmetric matrix. By symmetry of $\boldsymbol{\chi}$ we must have $\boldsymbol{\chi}_{\alpha\beta} = \boldsymbol{\chi}_{\beta\alpha}{}^T$.

### 4.5. The Covariance Matrix and Courant-Snyder Relations

Another quantity of interest is the *covariance matrix*, which is the matrix of central second moments. This matrix is akin to the standard deviation of single variable statistics. By a central moment, we mean that the moments are taken about the mean of the distribution. Thus, the covariance matrix $\boldsymbol{\sigma}$ is defined

$$(58)\qquad \boldsymbol{\sigma} \equiv \left\langle (\mathbf{z} - \bar{\mathbf{z}})(\mathbf{z} - \bar{\mathbf{z}})^T \right\rangle.$$

Note that by expanding the outer product of vectors then commuting the moment operator yields

$$(59)\qquad \boldsymbol{\sigma} = \boldsymbol{\chi} - \bar{\mathbf{z}}\bar{\mathbf{z}}^T.$$

Thus, we can determine the covariance matrix from the mean value vector and the correlation matrix. The covariance matrix has the block matrix form

$$\boldsymbol{\sigma} = \begin{pmatrix} \boldsymbol{\chi}_{\mathbf{xx}} - \mathbf{x}\mathbf{x}^T & \boldsymbol{\chi}_{\mathbf{xy}} - \mathbf{x}\mathbf{y}^T & \boldsymbol{\chi}_{\mathbf{xz}} - \mathbf{x}\boldsymbol{\zeta}^T & \mathbf{0} \\ \boldsymbol{\chi}_{\mathbf{yx}} - \mathbf{y}\mathbf{x}^T & \boldsymbol{\chi}_{\mathbf{yy}} - \mathbf{y}\mathbf{y}^T & \boldsymbol{\chi}_{\mathbf{yz}} - \mathbf{y}\boldsymbol{\zeta}^T & \mathbf{0} \\ \boldsymbol{\chi}_{\mathbf{zx}} - \boldsymbol{\zeta}\mathbf{x}^T & \boldsymbol{\chi}_{\mathbf{zy}} - \boldsymbol{\zeta}\mathbf{y}^T & \boldsymbol{\chi}_{\mathbf{zz}} - \boldsymbol{\zeta}\boldsymbol{\zeta}^T & \mathbf{0} \\ \mathbf{0} & \mathbf{0} & \mathbf{0} & 0 \end{pmatrix}, \tag{60}$$

where $\mathbf{0}$ is the two-vector of zeros. Note that when the beam is centered, that is when $\bar{\mathbf{z}} = 0$, the covariance matrix and the correlation matrix are the same save for a value 1 in the constant coordinate entry.

When the motion is uncoupled between phase planes, $\boldsymbol{\sigma}$ has the simplified block-diagonal form

$$\boldsymbol{\sigma} = \begin{pmatrix} \boldsymbol{\sigma}_{\mathbf{xx}} & 0 & \cdots & 0 \\ 0 & \boldsymbol{\sigma}_{\mathbf{yy}} & & \vdots \\ \vdots & & \boldsymbol{\sigma}_{\mathbf{zz}} & \vdots \\ 0 & \cdots & \cdots & 0 \end{pmatrix}, \tag{61}$$

where each $\boldsymbol{\sigma}_{\alpha\alpha}$ is the 2×2 sub-covariance matrix for the $\alpha$ phase plane and $\mathbf{0}$ is the 2×2 zero matrix. In this situation the covariance matrix can be expressed in terms of the Courant-Snyder parameters. Or rather, we can view the Courant-Snyder parameters as an alternate parameterization of the independent covariance matrices $\boldsymbol{\sigma}_{\alpha\alpha}$. Referring to Eqs. (48) for a centered beam, the covariance matrices $\boldsymbol{\sigma}_{\mathbf{xx}}$ for the separate phase planes can be written

$$\boldsymbol{\sigma}_{\mathbf{xx}} = \begin{pmatrix} \beta_x \tilde{\varepsilon}_x & -\alpha_x \tilde{\varepsilon}_x \\ -\alpha_x \tilde{\varepsilon}_x & \gamma_x \tilde{\varepsilon}_x \end{pmatrix}, \quad \boldsymbol{\sigma}_{\mathbf{yy}} = \begin{pmatrix} \beta_y \tilde{\varepsilon}_y & -\alpha_y \tilde{\varepsilon}_y \\ -\alpha_y \tilde{\varepsilon}_y & \gamma_y \tilde{\varepsilon}_y \end{pmatrix}, \quad \boldsymbol{\sigma}_{\mathbf{zz}} = \begin{pmatrix} \beta_z \tilde{\varepsilon}_z & -\alpha_z \tilde{\varepsilon}_z \\ -\alpha_z \tilde{\varepsilon}_z & \gamma_z \tilde{\varepsilon}_z \end{pmatrix}. \tag{62}$$

Thus, given the Courant-Snyder parameters describing a beam we can construct the uncoupled phase covariance matrix in Eq. (61) using Eqs. (62). From there, given the location of the beam centroid in phase space $\bar{\mathbf{z}}$ we can form the correlation matrix by solving Eq. (59) for $\boldsymbol{\chi}$ to yield

$$\boldsymbol{\chi} = \boldsymbol{\sigma} + \bar{\mathbf{z}}\bar{\mathbf{z}}^T . \tag{63}$$

### 4.6. Linearization of the Self-Fields

It has been found that the evolution of the beam's second moments is determined primarily by the linear part of the forces [22]. The nonlinear parts are usually associated with emittance growth of the beam (see Section 4.1). In this analysis we consider only linear forces. We have already assumed that the external forces are linear according to machine design. The self-fields will, in general, have nonlinear components and, thus, the self-forces also will. Here we describe a linear approximation to the self-fields $E_x$, $E_y$, $E_z$ which is appropriate for our analysis.

Consider the self-field in the $x$-direction, $E_x$. We begin by assuming an expansion of the form

$$E_x(x) \approx a_0 + a_1 x . \tag{64}$$

where $a_0$ and $a_1$ are real numbers independent of $x$. Terms involving the other phase space coordinates (of the form $b_1 y$, $c_1 z$) are zero with the assumption of symmetry (see Section 5.1). One method of determining the coefficients $a_0$ and $a_1$ is by a minimum variance, or least squares, estimation technique [8][17]. Here we seek to minimize the norm of the error in the approximation, which is $\|E_x - a_0 - a_1 x\|$, $E_x$ being the actual self-field. In order that the expansion be most accurate in areas of higher beam concentration, we *choose* the norm $\|\cdot\|$ to be

$$\|g\| \equiv \left[ \int g^2(\mathbf{z})\, f(\mathbf{z}; s)\, d^6\mathbf{z} \right]^{1/2} = \left\langle g^2 \right\rangle^{1/2} . \tag{65}$$

It is easily checked that this is a valid norm for functions of the phase space coordinates. Using the least squares fitting technique, we are left with the following Gram system for the coefficients:

$$\begin{pmatrix} \langle 1 \rangle & \langle x \rangle \\ \langle x \rangle & \langle x^2 \rangle \end{pmatrix} \begin{pmatrix} a_0 \\ a_1 \end{pmatrix} = \begin{pmatrix} \langle E_x \rangle \\ \langle xE_x \rangle \end{pmatrix}. \tag{66}$$

The solution to this system is

$$a_0 = -\frac{\langle x \rangle}{\langle x^2 \rangle - \langle x \rangle^2} \langle xE_x \rangle, \qquad a_1 = \frac{1}{\langle x^2 \rangle - \langle x \rangle^2} \langle xE_x \rangle, \tag{67}$$

Thus, the electric field has the approximation

$$E_x \approx \frac{\langle xE_x \rangle}{\sigma_x^2} (x - \bar{x}). \tag{68}$$

We have analogous expressions for $E_y$ and $E_z$ so that all the field components have the following linear approximations:

$$E_x \approx \frac{\langle xE_x \rangle}{\langle x^2 \rangle - \langle x \rangle^2} (x - \bar{x}), \qquad E_y \approx \frac{\langle yE_y \rangle}{\langle y^2 \rangle - \langle y \rangle^2} (y - \bar{y}), \qquad E_z \approx \frac{\langle zE_z \rangle}{\langle z^2 \rangle - \langle z \rangle^2} (z - \bar{z}). \tag{69}$$

Note once again that these linear approximations to the true fields are most accurate in the regions of highest beam density. They are most useful when considering the collective behavior, or rms behavior, of the beam.

When the beam is centered on the origin in configuration space these expressions simplify. This situation can be achieved through a simple coordinate translation, which does not affect the shape of the electric field and, therefore, the moment $\langle xE_x \rangle$. When the beam is centered (i.e., when $\bar{x} = \bar{y} = \bar{z} = 0$ and $\sigma_x = \tilde{x}$) the values of the expansion coefficients are

$$a_0 = 0 \qquad \text{and} \qquad a_1 = \frac{\langle xE_x \rangle}{\langle x^2 \rangle}. \tag{70}$$

Thus, in this case

$$E_x \approx a_1 x = \frac{\langle xE_x \rangle}{\langle x^2 \rangle} x. \tag{71}$$

### 4.7. Tune Depression

To demonstrate the usefulness of the material in the previous section we digress somewhat to show how it is related to a common parameter in beam physics known as the *tune depression* $\eta$. Tune depression is a parameter indicating the relative effect of space charge compared to the effects of transverse focusing in a beam channel. To illustrate, return to the original equations of motion (21) for an individual particle. Employing the linear approximation to the self-field given by Eq. (71), the approximate equation of motion in the $x$-plane is

$$x'' + \frac{\gamma'}{\gamma} x' + \left( k_x^2 - K \frac{2\pi\varepsilon_0}{qN} a_1 \right) x = 0. \tag{72}$$

The square root of the quantity in parenthesis is known as the tune-depressed phase advance, or phase advance with space charge and is typically denoted $k$ in the literature. The quantity $k_x$ in the above is called the phase advance without space charge and is usually denoted $k_0$. We see that an immediate consequence

of space charge is the reduction of external focusing. Consequently, the frequency of the particles' betatron oscillations, or betatron tune, decreases with increasing space charge forces.

Tune depression $\eta$ is defined

(73) $$\eta \equiv k / k_0 .$$

It is the factor by which the betatron tune frequency is decreased, having a maximum value of 1 (no tune depression) and a minimum value approaching 0 (complete tune depression). Using the above expansion we find the tune depression (in the $x$ plane) to be

(74) $$\eta = \left[ 1 - \frac{K}{k_x^2} \frac{2\pi\varepsilon_0}{qN} \frac{\langle xE_x \rangle}{\langle x^2 \rangle} \right]^{1/2} = \left[ 1 - \frac{q}{\gamma^2 \kappa_x} \frac{\langle xE_x \rangle}{\langle x^2 \rangle} \right]^{1/2} .$$

From the above relation we see that the tune depression is a function of the self-fields, the beam energy, and the external fields.

## 5. Ellipsoidal Beams and the Equivalent Uniform Beam

Here we define and describe ellipsoidal beams. For these beams it is possible to compute the field moments $\langle xE_x \rangle$, $\langle yE_y \rangle$, $\langle zE_z \rangle$ analytically in terms of elliptical integrals. The results of these calculations lead to the concept of the equivalent uniform beam. This notion says that we may model any (ellipsoidal) beam, at least approximately, by a uniform density beam with the same second moments.

### 5.1. Ellipsoidally Symmetric Charge Density Distributions

We restrict our attention to ensemble distributions that are ellipsoidally symmetric in configuration space, that is, in $(x,y,z)$ space. For simplicity we assume an upright, centered ellipsoid at the origin. For an arbitrarily oriented ellipsoid we can always apply a change of coordinates to achieve this condition (see next section). In this situation the charge density $\rho(x,y,z)$ has the form

(75) $$\rho(x,y,z) = q\,F\left( \frac{x^2}{a^2} + \frac{y^2}{b^2} + \frac{z^2}{c^2} \right),$$

where $q$ is the unit charge, and $a$, $b$, $c$ represent the semi-axes of the reference ellipsoid in the $x$, $y$, $z$ directions respectively. The function $F(\cdot)$ represents the profile of the distribution and is related to the density function $f$ by

(76) $$F(x,y,z;s) \equiv \iiint_{\Re^3} f(x,x',y,y',z,z';s)\,dx'dy'dz' ,$$

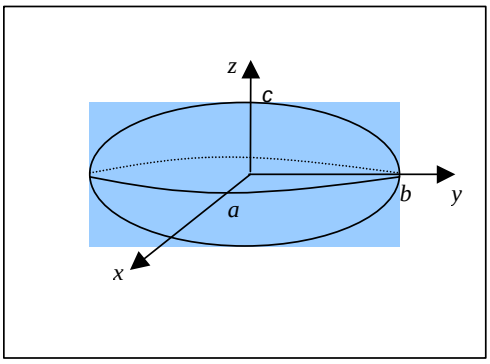

Figure 3: reference ellipsoid for ellipsoidally symmetric charge density

that is, we have integrated out the momentum dependence. This situation is depicted in Figure 3.

We compute the spatial moments of this distribution in order to find a relation between the moments, the total number of particles $N$, and the semi-axes $a$, $b$, $c$. For example, the total number of particles $N$ is

(77) $$N = \iiint_{\Re^3} F\left( \frac{x^2}{a^2} + \frac{y^2}{b^2} + \frac{z^2}{c^2} \right) dxdydz .$$

This integral may be computed by using the change of coordinates

$$
\begin{aligned}
&x = ar\sin\theta\cos\phi, \\
&y = br\sin\theta\sin\phi, \qquad dxdydz = abc\,r^2\sin\theta\,dr\,d\theta\,d\phi, \\
&z = cr\cos\theta,
\end{aligned}
\tag{78}
$$

with the result

$$
\begin{aligned}
N &= abc\int_0^{2\pi}\int_0^{\pi}\sin\theta\,d\theta\,d\phi\int_0^{\infty} r^2F(r^2)\,dr\,, \\
&= 2\pi abc\,F_{1/2}\,.
\end{aligned}
\tag{79}
$$

where $F_n$ is the $n^{\text{th}}$ moment of $F$, defined as

$$
F_n \equiv \int_0^{\infty} s^n F(s)\,ds\,. \tag{80}
$$

Note that $n$ is not restricted to integer values. Using a similar approach we can compute the following moments of the ellipsoidal distribution:

$$
\begin{aligned}
&\langle 1\rangle = 1, \\
&\langle x\rangle = \langle y\rangle = \langle z\rangle = 0, \\
&\langle x^2\rangle = \frac{a^2}{3}\frac{F_{3/2}}{F_{1/2}}, \\
&\langle y^2\rangle = \frac{b^2}{3}\frac{F_{3/2}}{F_{1/2}}, \\
&\langle z^2\rangle = \frac{c^2}{3}\frac{F_{3/2}}{F_{1/2}}.
\end{aligned}
\tag{81}
$$

These equations provide us expressions of the semi-axes $a$, $b$, $c$ in terms of the second spatial moments $\langle x^2\rangle$, $\langle y^2\rangle$, $\langle z^2\rangle$, respectively.

### 5.2. Arbitrarily Oriented Ellipsoidal Charge Densities

Here we consider ellipsoidal charge densities that are centered on the $xyz$ coordinate axes, however, they may have arbitrary orientation. The general representation of such a charge density is given by [3]

$$
\rho(x,y,z) = qF\left(\mathbf{r}^T\boldsymbol{\tau}^{-1}\mathbf{r}\right), \tag{82}
$$

where $\rho$, $q$, and $F$ are as in the previous section, $\mathbf{r}$ is the position vector in three space, that is,

$$
\mathbf{r} = (r_1 \quad r_2 \quad r_3) \equiv (x \quad y \quad z)^T\,, \tag{83}
$$

and

$$
\boldsymbol{\tau} \equiv \begin{pmatrix} \tau_{11} & \tau_{12} & \tau_{13} \\ \tau_{12} & \tau_{22} & \tau_{23} \\ \tau_{13} & \tau_{23} & \tau_{33} \end{pmatrix} \tag{84}
$$

is a symmetric, positive-definite matrix in $GL(3,\Re)$. (The motivation for representing $\rho$ using the inverse $\boldsymbol{\tau}^{-1}$ should become clear shortly.) Because of its symmetry, we can find a matrix $\mathbf{R}$ in the special orthogonal group $SO(3)$ that diagonalizes $\boldsymbol{\tau}$. That is,

$$
\boldsymbol{\tau} = \mathbf{R}\,\mathbf{D}\,\mathbf{R}^T\,, \tag{85}
$$

where $\mathbf{D}$ is the diagonal matrix of eigenvalues of $\boldsymbol{\tau}$, specifically

$$\text{(86)} \qquad \mathbf{D} \equiv \begin{pmatrix} \lambda_1 & 0 & 0 \\ 0 & \lambda_2 & 0 \\ 0 & 0 & \lambda_3 \end{pmatrix}$$

The eigenvalues $\lambda_1,\lambda_2,\lambda_3$ are the squares of the ellipsoid semi-axes (the values $a^2,b^2,c^2$ of the previous section). We can also find a set orthonormal (column) eigenvectors of $\boldsymbol{\tau}$ denoted $\{\mathbf{e}_1,\mathbf{e}_2,\mathbf{e}_3\}$. These eigenvectors may be used to build the matrix $\mathbf{R}$ as follows:

$$\text{(87)} \qquad \mathbf{R} = \begin{pmatrix} R_{1,1} & R_{1,2} & R_{1,3} \\ R_{2,1} & R_{2,2} & R_{2,3} \\ R_{3,1} & R_{3,2} & R_{3,3} \end{pmatrix} = \left(\mathbf{e}_1 \vdots \mathbf{e}_2 \vdots \mathbf{e}_3\right).$$

Recall that since $\mathbf{R}$ is in the special orthogonal group $SO(3)$ it has the following properties: $\mathbf{R}\mathbf{R}^T=\mathbf{1}$, $\mathbf{R}^{-1}=\mathbf{R}^T$, $\det(\mathbf{R})=1$.

To demonstrate the usefulness of the above facts we compute the total number of particles $N$ in the charge density

$$\text{(88)} \qquad \begin{aligned} N &= \iiint_{\Re^3} F(\mathbf{r}^T\boldsymbol{\tau}^{-1}\mathbf{r})\,d^3\mathbf{r}\,, \\ &= \iiint_{\Re^3} F\left((\mathbf{R}^T\mathbf{r})^T\mathbf{D}^{-1}(\mathbf{R}^T\mathbf{r})\right)d^3\mathbf{r}, \end{aligned}$$

where we have substituted $\boldsymbol{\tau}=\mathbf{R}\mathbf{D}\mathbf{R}^T$ in the second line. The parenthetical groupings suggest the following change of coordinates:

$$\text{(89)} \qquad \mathbf{r} = \mathbf{R}\mathbf{s}, \qquad \begin{aligned} d^3\mathbf{r} &= \det(\mathbf{R})\,d^3\mathbf{s}, \\ &= d^3\mathbf{s}\,, \end{aligned}$$

from which we get

$$\text{(90)} \qquad \begin{aligned} N &= \iiint_{\Re^3} F(\mathbf{s}\mathbf{D}^{-1}\mathbf{s})\,d^3\mathbf{s}, \\ &= \iiint_{\Re^3} F\left(\frac{s_1^2}{\lambda_1}+\frac{s_2^2}{\lambda_2}+\frac{s_3^2}{\lambda_3}\right)d^3\mathbf{s}. \end{aligned}$$

Now we have the expression for $N$ in the same form as we started with in the previous section. Thus, converting the integration to spherical coordinates using

$$\text{(91)} \qquad \begin{aligned} s_1 &= \sqrt{\lambda_1}\,r\sin\theta\cos\phi, \\ s_2 &= \sqrt{\lambda_2}\,r\sin\theta\sin\phi, \\ s_3 &= \sqrt{\lambda_3}\,r\cos\theta, \end{aligned} \qquad \begin{aligned} d^3\mathbf{s} &= \sqrt{\lambda_1\lambda_2\lambda_3}\;r^2\sin\theta\,dr d\theta d\phi, \\ &= \sqrt{\det\boldsymbol{\tau}}\;\;r^2\sin\theta\,dr\,d\theta\,d\phi, \end{aligned}$$

to find

$$\text{(92)} \qquad \begin{aligned} N &= \sqrt{\lambda_1\lambda_2\lambda_3}\int_0^{2\pi}\int_0^{\pi}\sin\theta\,d\theta\,d\phi\int_0^{\infty} r^2F(r^2)\,dr\,, \\ &= 2\pi\sqrt{\det\boldsymbol{\tau}}\,F_{1/2}\,. \end{aligned}$$

This result is the same as Eq. (79) of the last section if we identify $\det(\boldsymbol{\tau})=a^2b^2c^2$.

Another useful fact is that for the density distribution of Eq. (82), $\boldsymbol{\tau}$ is actually the matrix of all second-order moments. Specifically, we find that

$$\left\langle r_i r_j \right\rangle = \frac{1}{3}\tau_{ij}\frac{F_{3/2}}{F_{1/2}}. \tag{93}$$

To see this, start with the following expression

$$\left\langle r_i r_j \right\rangle = \frac{1}{N}\iiint_{\Re^3} r_i r_j F(\mathbf{r}^T\boldsymbol{\tau}^{-1}\mathbf{r})\,d^3\mathbf{r}, \tag{94}$$

then employ the orthogonal coordinate transform **r**=**Rs** of Eq. (89) to yield

$$\left\langle r_i r_j \right\rangle = \frac{1}{N}\sum_{m=1}^{3}\sum_{n=1}^{3}\iiint_{\Re^3}\left(R_{i,m}s_m\right)\left(R_{j,n}s_n\right)F(\mathbf{s}^T\mathbf{D}^{-1}\mathbf{s})\,d^3\mathbf{s}, \tag{95}$$

where we note that $r_i=\sum R_{i,m}s_m$ and $r_j=\sum R_{j,n}s_n$; $R_{i,m}$ and $R_{j,n}$ being the elements of the orthogonal matrix **R** in Eq (87). Switching to the spherical coordinates of Eq. (91) and performing the integration over $\phi$ produces

$$\begin{aligned}\left\langle r_i r_j \right\rangle &= \frac{\sqrt{\lambda_1\lambda_2\lambda_3}\,\pi}{N}\int_0^\infty r^4 F(r^2)dr\int_0^\pi\left[\lambda_1 R_{i,1}R_{j,1}\sin^3\theta+\lambda_2 R_{i,2}R_{j,2}\sin^3\theta+2\lambda_3 R_{i,3}R_{j,3}\cos^2\theta\sin\theta\right]d\theta,\\ &= \frac{\sqrt{\det\boldsymbol{\tau}}}{N}\frac{4\pi}{3}\int_0^\infty r^4 F(r^2)\,dr\;\tau_{i,j},\\ &= \frac{\tau_{ij}}{3}\frac{F_{3/2}}{F_{1/2}}.\end{aligned} \tag{96}$$

Thus we see that Eq. (93) is true.

### 5.3. Ellipsoidally Symmetric Phase Space Distributions

In the previous section we considered beam distributions that were ellipsoidally symmetric in configuration space. Here we generalize to the case where the distribution has hyper-ellipsoidal symmetry throughout all of phase space. This situation is equivalent to expressing the distribution function in terms of a quadratic form in the phase space variables. Specifically, if $\boldsymbol{\sigma}$ is the covariance matrix defined in Eq.(58), then the distribution function *f* has the form

$$f(x,x',y,y',z,z') = f\left(\mathbf{z}^T\boldsymbol{\sigma}^{-1}\mathbf{z}\right). \tag{97}$$

Using a similar approach as in the previous subsection, it can be shown that in this case any second order moment $\langle z_i z_j\rangle$ has the value (for a detailed exposition of this fact see [9])

$$\left\langle z_i z_j \right\rangle = \frac{1}{6}\sigma_{ij}\frac{f_3}{f_2} \tag{98}$$

where

$$f_n \equiv \int_0^\infty s^n f(s)\,ds, \tag{99}$$

and the $\sigma_{ij}$ are the elements of the covariance matrix $\boldsymbol{\sigma}$. The only exceptional variation from the previous procedure is employing six-dimensional hyper-spherical coordinates. To demonstrate their application, consider the calculation of the total number of particles *N* in the distribution

$$N = \int_{\Re^6} f(\mathbf{z}^T\boldsymbol{\sigma}^{=1}\mathbf{z})\,d^6\mathbf{z} \tag{100}$$

After rotating the coordinates by the diagonalizing matrix $\mathbf{R}\in SO(6)$ we have the decoupled integral

$$N = \int_{\Re^6} f(\mathbf{s}^T \mathbf{D}^{-1}\mathbf{s})\, d^6\mathbf{s}\,, \tag{101}$$

where $\mathbf{D}=\mathbf{R}^T\boldsymbol{\sigma}\mathbf{R}$ is the diagonal matrix of eigenvalues of $\boldsymbol{\sigma}$. Now apply the change of coordinates

$$\begin{aligned} s_1 &= \sqrt{\lambda_1}\, r\cos\theta_1\,, \\ s_2 &= \sqrt{\lambda_2}\, r\sin\theta_1\cos\theta_2\,, \\ s_3 &= \sqrt{\lambda_3}\, r\sin\theta_1\sin\theta_2\cos\theta_3\,, \\ s_4 &= \sqrt{\lambda_4}\, r\sin\theta_1\sin\theta_2\sin\theta_3\cos\theta_4\,, \\ s_5 &= \sqrt{\lambda_5}\, r\sin\theta_1\sin\theta_2\sin\theta_3\sin\theta_4\cos\phi\,, \\ s_6 &= \sqrt{\lambda_6}\, r\sin\theta_1\sin\theta_2\sin\theta_3\sin\theta_4\sin\phi\,, \end{aligned} \qquad d^6\mathbf{s} = r^5\, dr\, d\Omega, \tag{102}$$

where

$$d\Omega \equiv \sin^4\theta_1 \sin^3\theta_2 \sin^2\theta_3 \sin\theta_4\, d\theta_1\, d\theta_2\, d\theta_3\, d\theta_4\, d\phi\,, \tag{103}$$

is the solid angle in six dimensions. The total solid angle $\Omega$ in six dimensions is the surface area of the unit sphere given by

$$\begin{aligned} \Omega &= \int d\Omega = \int_0^\pi d\theta_1 \int_0^\pi d\theta_2 \int_0^\pi d\theta_3 \int_0^\pi d\theta_4 \int_0^{2\pi} d\phi \sin^4\theta_1 \sin^3\theta_2 \sin^2\theta_3 \sin\theta_4\,, \\ &= \pi^3 \end{aligned} \tag{104}$$

Thus, the total number of particles $N$ has the value

$$\begin{aligned} N &= \pi^3 \sqrt{\lambda_1\lambda_2\lambda_3\lambda_4\lambda_5\lambda_6} \int_0^\infty r^5 f(r^2)\, dr\,, \\ &= \frac{\pi^3}{2}\sqrt{\det\boldsymbol{\sigma}}\, f_2\,. \end{aligned} \tag{105}$$

Using Eq. (98) we can write an analogous expression to Eq. (45) for the entire rms phase space hyper-ellipsoid compactly in matrix-vector notation as

$$\mathbf{z}^T \boldsymbol{\chi}_{xx}^{-1} \mathbf{z} = \frac{\widetilde{\varepsilon}}{\det\boldsymbol{\chi}} \tag{106}$$

where $\widetilde{\varepsilon}$ is the hyper-volume of the entire six-dimension phase-space ellipsoid. Note that here it is necessary to normalize by the determinant of $\chi$ since its value is not required to be unity.

### 5.4. Computation of the Field Moments

It is possible to compute the field moments explicitly (in terms of elliptic integrals) for beams having ellipsoidal symmetry in configuration space. We start from the following formula for the self-electric potential of such a bunch [11][15]:

$$\phi(x,y,z) = \frac{qabc}{4\varepsilon_0} \int_0^\infty \int_{T(x,y,z;t)}^\infty \frac{F(s)}{\left(t+a^2\right)^{1/2}\left(t+b^2\right)^{1/2}\left(t+c^2\right)^{1/2}}\, ds\, dt\,, \tag{107}$$

where the limit of integration $T(x,y,z;t)$ is defined

$$T(x,y,z;t) \equiv \frac{x^2}{t+a^2} + \frac{y^2}{t+b^2} + \frac{z^2}{t+c^2}\,. \tag{108}$$

The formula assumes that the bunch is centered at the $(x,y,z)$ origin and that its semi-axes $a,b,c$ are aligned with the coordinate axes $x,y,z$ as shown in Figure 3. It is found by inverting Laplace's equation for $\phi$ in

ellipsoidal coordinates (the variable $t$ is actually an ellipsoidal coordinate). Using Eq. (107) the expressions for the field moments are computed to be (see Appendix A)

$$\begin{aligned}
\langle xE_x\rangle &= \Gamma(F)\frac{q\pi}{6\varepsilon_0}\frac{a^2b^2c^2}{N}a^2\,R_D(c^2,b^2,a^2)\,,\\
\langle yE_y\rangle &= \Gamma(F)\frac{q\pi}{6\varepsilon_0}\frac{a^2b^2c^2}{N}b^2\,R_D(a^2,c^2,b^2)\,,\\
\langle zE_z\rangle &= \Gamma(F)\frac{q\pi}{6\varepsilon_0}\frac{a^2b^2c^2}{N}c^2\,R_D(a^2,b^2,c^2)\,,
\end{aligned} \qquad (109)$$

$$G(r)\equiv\int_r^\infty F(s)\,ds\,,\qquad \Gamma(F)\equiv\int_0^\infty G^2(r^2)\,dr,$$

where $\Gamma$ carries the distribution information (it is a function of the profile $F$), and $R_D$ is the Carlson elliptic integral of the second kind [5][6].

Carlson's definitions for elliptic integrals are much more convenient in this situation. Moreover, they lend themselves nicely to numeric computation [19]. Definitions for these integrals are as follows:

$$\begin{aligned}
R_F(x,y,z) &\equiv \frac{1}{2}\int_0^\infty \frac{dt}{(t+x)^{1/2}(t+y)^{1/2}(t+z)^{1/2}}\,,\\
R_D(x,y,z) &\equiv \frac{3}{2}\int_0^\infty \frac{dt}{(t+x)^{1/2}(t+y)^{1/2}(t+z)^{3/2}}\,,\\
R_J(x,y,z,p) &\equiv \frac{3}{2}\int_0^\infty \frac{dt}{(t+x)^{1/2}(t+y)^{1/2}(t+z)^{1/2}(t+p)}.
\end{aligned} \qquad (110)$$

Note that only $R_F$ is symmetric in its arguments. It is possible to express all the conventional elliptic integrals ($E$, $F$, $K$, etc.) in terms of $R_F$, $R_D$ and $R_J$.

### 5.5. The Equivalent Uniform Beam

We would prefer to express Eqs. (109) in a form independent of the parameters $a$, $b$, $c$. Rather we could use the variables $\langle x^2\rangle$, $\langle y^2\rangle$, $\langle z^2\rangle$ by employing the relations (81). First note that

$$R_D(x,y,z) = r^{3/2}R_D(rx,ry,rz) \qquad (111)$$

for any positive real number $r$. Thus, choosing $r=1/c^2$ we have

$$R_D(a^2,b^2,c^2) = \frac{1}{c^3}R_D\left[\frac{a^2}{c^2},\frac{b^2}{c^2},1\right]. \qquad (112)$$

Using this property of $R_D$ we can express the self-moments as

$$\begin{aligned}
\langle xE_x\rangle &= \frac{\Lambda(F)}{\sqrt{3}}\frac{Q}{24\pi\varepsilon_0}\frac{1}{<x^2>^{1/2}}R_D\left[\frac{<y^2>}{<x^2>},\frac{<z^2>}{<x^2>},1\right]\,,\\
\langle yE_y\rangle &= \frac{\Lambda(F)}{\sqrt{3}}\frac{Q}{24\pi\varepsilon_0}\frac{1}{<y^2>^{1/2}}R_D\left[\frac{<x^2>}{<y^2>},\frac{<z^2>}{<y^2>},1\right],\\
\langle zE_z\rangle &= \frac{\Lambda(F)}{\sqrt{3}}\frac{Q}{24\pi\varepsilon_0}\frac{1}{<z^2>^{1/2}}R_D\left[\frac{<x^2>}{<z^2>},\frac{<y^2>}{<z^2>},1\right],
\end{aligned} \qquad (113)$$

where the functional $\Lambda(F)$ is defined as

$$\Lambda(F) \equiv \Gamma(F)\frac{(F_{3/2})^{1/2}}{(F_{1/2})^{5/2}} = \int_0^\infty G^2(r^2)dr\frac{\left[\int_0^\infty r^{3/2}F(r)dr\right]^{1/2}}{\left[\int_0^\infty r^{1/2}F(r)dr\right]^{5/2}}. \tag{114}$$

The functional $\Lambda$ accounts for the effects of the particular beam distribution profile on the beam dynamics.

Table 1: Ellipsoidally symmetric profiles $F$ and the corresponding $\Lambda(F)$. The quantity $C$ represents an arbitrary constant.

| Distribution | $F(s)$ | $\Lambda(F)$ |
|---|---|---|
| **Uniform** | $\begin{cases} C & s \le 1 \\ 0 & s > 1 \end{cases}$ | $\frac{6}{5}\sqrt{\frac{3}{5}} \approx 0.9295$ |
| **Parabolic (Waterbag)** | $\begin{cases} C(1-s) & s \le 1 \\ 0 & s > 1 \end{cases}$ | $\frac{10}{7}\sqrt{\frac{3}{7}} \approx 0.9352$ |
| **Hollow** | $Cse^{-\frac{s}{2\sigma^2}}$ | $\frac{3}{4}\sqrt{\frac{5}{\pi}} \approx 0.9462$ |
| **Gaussian** | $Ce^{-\frac{s}{2\sigma^2}}$ | $\sqrt{\frac{3}{\pi}} \approx 0.9772$ |

Sacherer discovered that the functional $\Lambda$ is nearly constant with respect to the distribution $F$ [22]. Table 1 lists the values of $\Lambda$ for several common distributions. We see there that its value varies only by about 5% for the distributions listed. The implication is that the second-order spatial moments (i.e., the rms envelopes) of any bunched beam behave approximately the same, irrespective of the particular beam profile. In other words, the beam dynamics are only loosely coupled to the actual form of the distribution, so long as it is ellipsoidal. Consequently, we are justified in modeling any laboratory beam with any other beam having the same second moments $\langle x^2\rangle$, $\langle y^2\rangle$ and $\langle z^2\rangle$. This notion leads to the concept of the *equivalent uniform beam*. This bean is the uniform density beam having the same second moment as the actual laboratory beam. Since the uniform beam has well-defined boundaries, this distribution is typically preferred. The moments in this case can be written as

$$\begin{aligned}
\left\langle xE_x\right\rangle &= \frac{1}{5^{3/2}}\frac{Q}{4\pi\varepsilon_0} < x^2 > R_D\left[< y^2 >, < z^2 >, < x^2 >\right] , \\
\left\langle yE_y\right\rangle &= \frac{1}{5^{3/2}}\frac{Q}{4\pi\varepsilon_0} < y^2 > R_D\left[< x^2 >, < z^2 >, < y^2 >\right] , \\
\left\langle zE_z\right\rangle &= \frac{1}{5^{3/2}}\frac{Q}{4\pi\varepsilon_0} < z^2 > R_D\left[< x^2 >, < y^2 >, < z^2 >\right] ,
\end{aligned} \tag{115}$$

where we have used the relation

$$R_D\left(X^2, Y^2, Z^2\right) = \frac{1}{Z^3}R_D\left[\frac{X^2}{Z^2}, \frac{Y^2}{Z^2}, 1\right]. \tag{116}$$

Finally, we note in passing that in the case of continuous elliptic beams, the dynamics are completely independent of the beam profile.

Recognize that the semi-axes of the reference ellipsoid $a$, $b$, $c$, are actually the envelopes of the uniform beam. This being so, we can use Eqs. (81) to relate the envelopes of the uniform beam and the second spatial moments. It is common in the literature to denote the envelopes of the equivalent uniform

beam by $X$, $Y$, $Z$ corresponding to the semi-axes $a$, $b$, $c$, respectively. Thus, for the equivalent uniform ellipsoid we have

$$(117) \qquad X = \left[5\left\langle x^2 \right\rangle\right]^{1/2} = \sqrt{5}\tilde{x} \qquad Y = \left[5\left\langle y^2 \right\rangle\right]^{1/2} = \sqrt{5}\tilde{y} \qquad Z = \left[5\left\langle z^2 \right\rangle\right]^{1/2} = \sqrt{5}\tilde{z} \,.$$

Likewise, it is common to define the *effective emittance* $\varepsilon$ of the equivalent uniform beam in terms of the rms emittance according to the following:

$$(118) \qquad \varepsilon_x \equiv 5\tilde{\varepsilon}_x \qquad \varepsilon_y \equiv 5\tilde{\varepsilon}_y \qquad \varepsilon_z \equiv 5\tilde{\varepsilon}_z \,.$$

The effective emittances represent the areas in the phase planes occupied by the equivalent uniform beam.

We can also determine the second-order moments of the equivalent uniform ellipsoid using their definitions (117) and the definition of rms emittance (37). For the $x$-plane we find

$$(119) \qquad \begin{aligned} \left\langle x^2 \right\rangle &= \frac{1}{5} X^2 \,, \\ \left\langle xx' \right\rangle &= \frac{1}{5} XX' \,, \\ \left\langle x'^2 \right\rangle &= \frac{1}{5} X'^2 + \frac{5\tilde{\varepsilon}_x^2}{X^2} \,, \end{aligned}$$

where $X'=dX/ds$ is the rate of change of the equivalent beam envelope with respect to $s$. There are analogous relations for the other phase planes.

The envelope $X$ of the equivalent uniform ellipsoid can be expressed in terms of the Courant-Snyder parameters through inspection of the extremal points of the trace-space ellipse (for example, see Reiser [24]). The result is

$$(120) \qquad \begin{aligned} X &= \sqrt{5\beta_x \tilde{\varepsilon}_x} \,, \\ X' &= -\alpha_x \sqrt{\frac{5\tilde{\varepsilon}}{\beta_x}} \,. \end{aligned}$$

There are similar expressions for the $y$ and $z$ phase planes.

## 6. BUNCHED BEAM ENVELOPE EQUATIONS

The final result of this section is a set of coupled ordinary differential equations describing the evolution of the equivalent uniform beam, given by Eqs. (124). Although nonlinear, these equations are a relatively simple set of ordinary differential equations that may be integrated numerically using standard techniques. The shortcoming of this description is that, aside from space charge, it does not account for external coupling between phase planes. That is, coupling such as that from misaligned quadrupoles, skew elements, etc., cannot be modeled. This drawback is circumvented in the follow section on transfer matrix methods by considering all the second-order moments.

### 6.1. Equations for Centroid Motion

The equations for the first-order moments are simply the equations of motion for the centroid of the beam, which behaves as a single particle. The evolution equations for the average values are found with reference to Eqs. (30). By differentiating the first equation of each set in Eqs. (30) then substituting into the second we find

$$
\begin{aligned}
&\bar{x}'' + \frac{\gamma'}{\gamma}\bar{x}' + k_x^2 \bar{x} = 0, \\
&\bar{y}'' + \frac{\gamma'}{\gamma}\bar{y}' + k_y^2 \bar{y} = 0, \\
&\bar{z}'' + \frac{\gamma'}{\gamma}\bar{z}' + k_z^2 \bar{z} = -\frac{\gamma'}{\gamma},
\end{aligned}
\tag{121}
$$

which are a closed set involving only $\bar{x}, \bar{y}, \text{and } \bar{z}$. They are damped harmonic equations and may be solved independently by standard techniques. Recall that the $k_\alpha^2$ are functions of $s$ and that it is possible for $k_\alpha^2$ to be negative, that is, $\kappa_\alpha$ is negative.

### 6.2. Bunched Beam RMS Envelope Equations

Here we develop a set of coupled ordinary differential equations that describe the evolution of the rms envelopes of the beam, specifically the quantities $\tilde{x}, \tilde{y}, \tilde{z}$. These equations describe the behavior of the beam extent in a statistical sense. They can then be used to derive the equations for the equivalent uniform beam, as is done in the following subsection.

From the second-order moment equations (31) we can derive equations involving only the quantities $\tilde{x}, \tilde{y}, \tilde{z}$. Recall that $\tilde{x} \equiv \langle x^2 \rangle^{1/2}$. If we differentiate $\tilde{x}$ twice with respect to $s$ then use the relations (31) and the definition of rms emittance (37) we find a second-order differential equation for $\tilde{x}$. Proceeding in an analogous manner for the $y$ and $z$ planes we are left with the following set of ordinary differential equations:

$$
\begin{aligned}
&\tilde{x}'' + \frac{\gamma'}{\gamma}\tilde{x}' + k_x^2 \tilde{x} - K\frac{2\pi\varepsilon_0}{qN}\frac{\langle xE_x \rangle}{\tilde{x}} - \frac{\tilde{\varepsilon}_x^2}{\tilde{x}^3} = 0, \\
&\tilde{y}'' + \frac{\gamma'}{\gamma}\tilde{y}' + k_y^2 \tilde{y} - K\frac{2\pi\varepsilon_0}{qN}\frac{\langle yE_y \rangle}{\tilde{y}} - \frac{\tilde{\varepsilon}_y^2}{\tilde{y}^3} = 0, \\
&\tilde{z}'' + \frac{\gamma'}{\gamma}\tilde{z}' + k_z^2 \tilde{z} - \gamma^2 K\frac{2\pi\varepsilon_0}{qN}\frac{\langle zE_z \rangle}{\tilde{z}} - \frac{\tilde{\varepsilon}_z^2}{\tilde{z}^3} = -\frac{\gamma'}{\gamma}\bar{z}\,.
\end{aligned}
\tag{122}
$$

Note that these equations involve the moments $\langle xE_x \rangle$, $\langle yE_y \rangle$, $\langle zE_z \rangle$. As we have seen, these moments are generally functions of the $\tilde{x}, \tilde{y}, \tilde{z}$; so the above set form a coupled set of ordinary differential equations. Thus, once we determine the field moments we can solve the system using standard techniques (e.g., numerically). As they stand, these equations are valid for all beam distributions. In the next subsection we consider ellipsoidally symmetric beam distributions.

### 6.3. Ellipsoidally Symmetric Beams and the Equivalent Uniform Beam

Here we substitute the values $\langle xE_x \rangle$, $\langle yE_y \rangle$, $\langle zE_z \rangle$ that we calculated for beams with ellipsoidal symmetry into the above rms envelope equations (122). The result is

$$
\begin{aligned}
&\tilde{x}'' + \frac{\gamma'}{\gamma}\tilde{x}' + k_x^2 \tilde{x} - \frac{\Lambda(F)}{\sqrt{3}}\frac{K}{12}\frac{1}{\tilde{x}^2} R_D\left[\frac{\tilde{y}^2}{\tilde{x}^2}, \frac{\tilde{z}^2}{\tilde{x}^2}, 1\right] - \frac{\tilde{\varepsilon}_x^2}{\tilde{x}^3} = 0, \\
&\tilde{y}'' + \frac{\gamma'}{\gamma}\tilde{y}' + k_y^2 \tilde{y} - \frac{\Lambda(F)}{\sqrt{3}}\frac{K}{12}\frac{1}{\tilde{y}^2} R_D\left[\frac{\tilde{x}^2}{\tilde{y}^2}, \frac{\tilde{z}^2}{\tilde{y}^2}, 1\right] - \frac{\tilde{\varepsilon}_y^2}{\tilde{y}^3} = 0, \\
&\tilde{z}'' + \frac{\gamma'}{\gamma}\tilde{z}' + k_z^2 \tilde{z} - \gamma^2\frac{\Lambda(F)}{\sqrt{3}}\frac{K}{12}\frac{1}{\tilde{z}^2} R_D\left[\frac{\tilde{x}^2}{\tilde{z}^2}, \frac{\tilde{y}^2}{\tilde{z}^2}, 1\right] - \frac{\tilde{\varepsilon}_z^2}{\tilde{z}^3} = -\frac{\gamma'}{\gamma}\bar{z}.
\end{aligned}
\tag{123}
$$

These are the rms envelope equations for bunched beams with ellipsoidal symmetry.

Now consider the equivalent uniform beam. Substituting the value of $\Lambda$ for the equivalent uniform ellipsoid and using relations (117) and (118) we have

$$
\begin{aligned}
&X'' + \frac{\gamma'}{\gamma'} X' + k_x^2(s) X - \frac{K}{2} X\, R_D(Z^2, Y^2, X^2) - \frac{\varepsilon_x^2}{X^3} = 0\,, \\
&Y'' + \frac{\gamma'}{\gamma'} Y' + k_y^2(s) Y - \frac{K}{2} Y\, R_D(X^2, Z^2, Y^2) - \frac{\varepsilon_y^2}{Y^3} = 0\,, \\
&Z'' + \frac{\gamma'}{\gamma'} Z' + k_z^2(s) Z - \gamma^2 \frac{K}{2} Z\, R_D(X^2, Y^2, Z^2) - \frac{\varepsilon_z^2}{Z^3} = -\sqrt{5}\,\frac{\gamma'}{\gamma'}\,\bar{z}\,,
\end{aligned}
\tag{124}
$$

where we have used relation (111) to eliminate the fractional arguments in the elliptical integrals. When doing numerical computation, however, using the rational arguments for the elliptical integrals is probably more stable. For example, from Eq. (111) it is probably best to compute $R_D(X^2,Y^2,Z^2)$ as

$$
R_D\left(X^2, Y^2, Z^2\right) = \frac{1}{Z^3} R_D\left[\frac{X^2}{Z^2}, \frac{Y^2}{Z^2}, 1\right]. \tag{125}
$$

### 6.4. Approximate Form of the Envelope Equations

In the literature, the bunched beam envelope equations are sometimes expressed without explicit reference to elliptic integrals, typically by introduction of a "form factor" and/or approximations in lieu of the integrals [13]. There, we see algebraic expressions or expressions involving elementary functions instead of the special functions. One way to achieve this form is with the procedure given below. The approximation presented here is accurate when the transverse plane envelopes $X$ and $Y$ are approximately equal.

To simplify the discussion below, we begin by immediately introducing the *form factor* $\xi$. It is defined by

$$
\begin{aligned}
\xi(s) &\equiv \frac{s}{2}\int_0^\infty \frac{dt}{(t+1)\left(t+s^2\right)^{3/2}} \\
&= \frac{1}{1-s^2}\begin{cases} 1 - \dfrac{s}{\sqrt{1-s^2}}\cos^{-1} s & \text{for } s<1 \\ 1 - \dfrac{s}{\sqrt{s^2-1}}\cosh^{-1} s & \text{for } s>1 \end{cases}
\end{aligned}
\tag{126}
$$

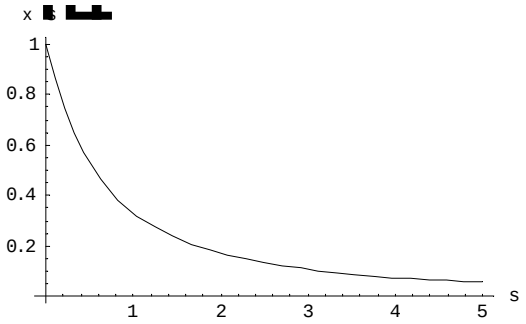


Figure 4: form factor $\xi$(s)

A plot of this function is shown in Figure 4. From the figure we see that $\xi$ has a value of 1 at $s$=0, 1/3 at $s$=1, then asymptotes toward zero as $s$ approaches infinity. Note that $\xi$ has the definition given by the integral expression, however, this integral may be expressed analytically in terms of elementary functions according to the above.

Using the form factor we can approximate the elliptic integrals by the following:

$$
\begin{aligned}
R_D(Z^2, Y^2, X^2) &\approx \frac{3}{XZ}\frac{1}{X+Y}\left[1 - \xi\left(\frac{Z}{\sqrt{XY}}\right)\right], \\
R_D(Z^2, X^2, Y^2) &\approx \frac{3}{YZ}\frac{1}{X+Y}\left[1 - \xi\left(\frac{Z}{\sqrt{XY}}\right)\right], \\
R_D(X^2, Y^2, Z^2) &\approx \frac{3}{XYZ}\,\xi\left(\frac{Z}{\sqrt{XY}}\right),
\end{aligned}
\tag{127}
$$

where the approximations are most accurate when $X \approx Y$, that is, the axisymmetric case. Substituting the approximations for the elliptic integral into the envelope equations for the equivalent uniform ellipsoid (124) yields the *approximate* envelope equations for the equivalent beam. They appear as follows:

$$\begin{aligned} &X'' + \frac{\gamma'}{\gamma} X' + k_x^2(s) X - \frac{3K}{2} \frac{1 - \xi(Z/\sqrt{XY})}{Z(X+Y)} - \frac{\varepsilon_x^2}{X^3} = 0 , \\ &Y'' + \frac{\gamma'}{\gamma} Y' + k_y^2(s) Y - \frac{3K}{2} \frac{1 - \xi(Z/\sqrt{XY})}{Z(X+Y)} - \frac{\varepsilon_y^2}{Y^3} = 0 , \\ &Z'' + \frac{\gamma'}{\gamma} Z' + k_z^2(s) Z - \gamma^2 \frac{3K}{2} \frac{\xi(Z/\sqrt{XY})}{XY} - \frac{\varepsilon_z^2}{Z^3} = -\sqrt{5} \frac{\gamma'}{\gamma'} \bar{z} , \end{aligned} \tag{128}$$

where we note the rational argument of the form factor $\xi$.

For the reminder of this subsection we confirm the approximations of Eqs. (127). We begin by performing an expansion of the *x* and *y* envelopes *X*, *Y* about their axisymmetric value *R*. Employing a small perturbation parameter $\varepsilon << 1$ (not to be confused with beam emittance) we have

$$\begin{aligned} X &= R + \varepsilon X_1 + \varepsilon^2 X_2 + \dots , \\ Y &= R + \varepsilon Y_1 + \varepsilon^2 Y_2 + \dots \ . \end{aligned} \tag{129}$$

With this expansion, note that

$$R = \frac{X+Y}{2} + O(\varepsilon) \qquad \text{and} \qquad \lim_{\varepsilon \to 0} \frac{X-Y}{\varepsilon} = X_1 - Y_1 . \tag{130}$$

That is, *R* can be interpreted as the average value of *X* and *Y* to first order. The perturbation parameter allows us to keep track of the order of accuracy in our approximations. As $\varepsilon$ increases the beam may become increasingly more eccentric in the transverse plane. In fact, our final results for this section are exact for axisymmetric beams.

Consider the envelope equation for the *z* plane. Writing out the elliptic integral explicitly in this case gives the following expression:

$$R_D(X^2, Y^2, Z^2) = \frac{3}{2} \frac{1}{(XY)^{3/2}} \int_0^\infty \frac{dt}{\sqrt{(t + X/Y)(t + Y/X)}\left(t + Z^2/XY\right)^{3/2}} , \tag{131}$$

where we have pulled a factor *XY* from each product in the denominator, then applied a change of variables. The expression under the radical can be written $t^2 + (X/Y + Y/X)t + 1$ with the term in parenthesis expanded as

$$\left(\frac{X}{Y} + \frac{Y}{X}\right) = 2 + \frac{(X_1 - Y_1)^2}{R^2} \varepsilon^2 + O(\varepsilon^4) . \tag{132}$$

Thus,

$$\sqrt{t^2 + (X/Y + Y/X)t + 1} = (t+1) + O(\varepsilon^2) \tag{133}$$

and we can approximate the elliptic integral as

$$\begin{aligned} R_D(X^2, Y^2, Z^2) &\approx \frac{3}{2} \frac{1}{XYZ} \frac{Z}{\sqrt{XY}} \int_0^\infty \frac{dt}{(t+1)\left(t + Z^2/XY\right)^{3/2}} , \\ &= \frac{3}{XYZ} \xi\left(\frac{Z}{\sqrt{XY}}\right) \end{aligned} \tag{134}$$

where we have identified the form factor $\xi(\cdot)$.

Now consider the transverse plane, in particular, the *x* plane. Results for the *y* plane follow in an analogous manner. The elliptic integral can be written

$$R_D(Z^2,Y^2,X^2)=\frac{3}{2}\frac{1}{(XY)^{3/2}}\int_0^\infty \frac{dt}{(t+Z/XY)^{1/2}(t+Y/X)^{1/2}(t+X/Y)^{3/2}}, \tag{135}$$

where, again, we have pulled a factor *XY* from each product in the denominator, then applied a change of variables. Now we expand the last two terms in the denominator as

$$\begin{aligned}(t+Y/X)^{1/2}(t+X/Y)^{1/2}(t+X/Y)&=(t+1)(t+X/Y)+O(\varepsilon^2),\\ &=(t+1)(1/Y)(tY+X)+O(\varepsilon^2),\\ &=\frac{R}{Y}(t+1)^2+O(\varepsilon),\\ &=\frac{1}{2Y}(X+Y)(t+1)^2+O(\varepsilon).\end{aligned} \tag{136}$$

Thus, we can approximate the elliptic integral as

$$\begin{aligned}R_D(Z^2,Y^2,X^2)&\approx\frac{3}{XZ}\frac{1}{(X+Y)}\frac{Z}{\sqrt{XY}}\int_0^\infty\frac{dt}{(t+Z^2/XY)^{1/2}(t+1)^2},\\ &=\frac{3}{XZ}\frac{1}{(X+Y)}\eta\left(\frac{Z}{\sqrt{XY}}\right)\end{aligned} \tag{137}$$

where the auxiliary function $\eta(\cdot)$ is defined

$$\begin{aligned}\eta(s)&\equiv\int_0^\infty\frac{s\,dt}{(t+s^2)^{1/2}(t+1)^2},\\ &=1-\xi(s).\end{aligned} \tag{138}$$

The equality on the second line is found through integration by parts. From this second relation we can express the elliptic integral for the transverse plane in terms of the original form factor

$$R_D(Z^2,Y^2,X^2)\approx\frac{3}{XZ}\frac{1}{X+Y}\left[1-\xi\left(\frac{Z}{\sqrt{XY}}\right)\right]. \tag{139}$$

Likewise, for the *y* plane we have

$$R_D(Z^2,X^2,Y^2)\approx\frac{3}{YZ}\frac{1}{X+Y}\left[1-\xi\left(\frac{Z}{\sqrt{XY}}\right)\right]. \tag{140}$$

Notice that our approximations for the transverse plane elliptic integrals are only accurate to order $\varepsilon$ whereas the longitudinal plane approximation is accurate to order $\varepsilon^2$. This condition makes sense in that the transverse plane approximations are more sensitive to the eccentricity in *X* and *Y* than the longitudinal approximation.

## 7. TRANSFER MATRIX APPROACH

Here we assume that, to first order, the dynamics of each beamline element *n* can be represented by a matrix $\mathbf{\Phi_n}$, known as the transfer matrix for the element. Thus, the action of the element on a particle with phase space coordinates $\mathbf{z}$ would be given by the matrix-vector product $\mathbf{\Phi_n z}$. In many situations it is possible to explicitly calculate the transfer matrix for a particular beamline element *a priori*, either analytically or numerically using the principles of linear systems. Moreover, it is found that, with a conjugation operation, the rms moments of the beam can be propagated using the same transfer matrix $\mathbf{\Phi_n}$.

For practical numerical simulation we usually separate the action of the external elements and the space charge effects. That is, the beam is propagated through the element according to its external forces, and corrections are applied to account for the space charge along the way. We find that it is possible to represent the action of the linearized space charge forces as a transfer matrix. Consequently, simulating the evolution of the moments up to second order requires determination of the transfer matrices for each beamline element and the transfer matrix that accounts for space charge.

### 7.1. Transfer Matrices and External Elements

Ignore space charge for the moment. Referring to Eqs. (21), the equations of motion for the $x$ plane can then be put into the matrix-vector form

$$\mathbf{x}'(s) = \mathbf{A}(s)\mathbf{x}(s)\,, \tag{141}$$

where

$$\mathbf{x}(s) \equiv \begin{pmatrix} x(s) \\ x'(s) \end{pmatrix} \quad \text{and} \quad \mathbf{A}(s) \equiv \begin{pmatrix} 0 & 1 \\ -k_x^2(s) & -\dfrac{\gamma'(s)}{\gamma(s)} \end{pmatrix}. \tag{142}$$

In principle, if we know $k_x^2(s)$ and $\gamma(s)$ there always exists a solution to Eq. (141) of the form [10]

$$\mathbf{x}(s) = \mathbf{\Phi}(s)\mathbf{x}(0)\,, \tag{143}$$

where $\mathbf{x}(0)$ is the initial value of $\mathbf{x}(s)$, and $\mathbf{\Phi}(s)$ is the *fundamental matrix* of the system; it is a matrix function of the independent variable $s$ having the following properties:

$$\begin{aligned} &\mathbf{\Phi}'(s) = \mathbf{A}(s)\mathbf{\Phi}(s), \\ &\mathbf{\Phi}(0) = \mathbf{I}, \end{aligned} \tag{144}$$

where $\mathbf{I}$ is the identity matrix. We use this fact to develop a numerical algorithm for simulation. If we determine the matrix $\mathbf{\Phi}$ for each beamline element (say by explicit calculation or by numerical integration of the above equation for $\mathbf{\Phi}$), then the particle coordinates can be propagated by simple matrix

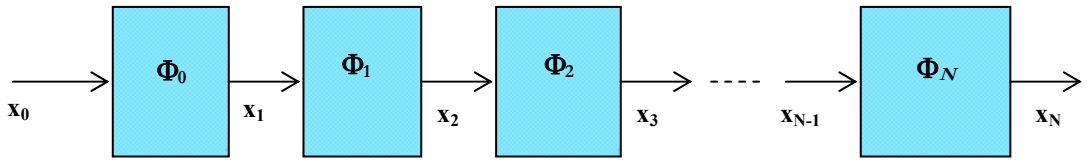


Figure 5: transfer matrix representation of the beamline

multiplication. (This fact comes from the semi-group property of the fundamental matrix.)

We can discretize the continuous matrix-vector system (143) by considering only points at the entrance and exit locations of each beamline element. Let $\mathbf{\Phi_n}$ denote the fundamental matrix solution for beamline element $n$ having length $l_n$ evaluated at the final location, that is

$$\mathbf{\Phi}_n \equiv \mathbf{\Phi}(l_n) \tag{145}$$

The constant matrix $\mathbf{\Phi_n}$ is known as the *transfer matrix* for the element $n$. Now let $\mathbf{x_n}$ denote the state of the particle at the entrance of the $n^{\text{th}}$ beamline element

(146) $\mathbf{x_n} \equiv \mathbf{x}(s_n)$,

where $s_n$ is the location of the $n^{\text{th}}$ element's entrance. This situation is shown in Figure 5. Propagation of the particle state from one element to the next is given by the set of discrete equations

(147) $\mathbf{x}_{n+1} = \mathbf{\Phi}_n \mathbf{x}_n \qquad n = 0,1,\ldots$

Thus, instead of a set of continuous ordinary differential equations we now have a set of discrete *transfer equations* to describe the particle motion. By the linearity of electromagnet forces we can describe the action of each element by its transfer matrix $\mathbf{\Phi_n}$ then use a separate process to determine the space-charge effects down the beamline.

Many times we can compute the transfer matrix for a beamline element analytically. For example, in the case of an ideal quadrupole lens where the forces are linear throughout and the fringe fields are negligible, then the transfer matrix is found to be

(148) $$\mathbf{\Phi_{quad}} = \begin{pmatrix} \cos kl & \frac{1}{k}\sin kl & 0 & 0 & 0 & 0 \\ -k\sin kl & \cos kl & 0 & 0 & 0 & 0 \\ 0 & 0 & \cosh kl & \frac{1}{k}\sinh kl & 0 & 0 \\ 0 & 0 & k\sinh kl & \cosh kl & 0 & 0 \\ 0 & 0 & 0 & 0 & 1 & l \\ 0 & 0 & 0 & 0 & 0 & 1 \end{pmatrix},$$

where $k$ is the quadrupole focusing strength, $l$ is the length of the quadrupole, and where the quadrupole is focusing in $x$ and defocusing in $y$. Note that in this ideal case there is no coupling between phase planes. A description including misalignments would contain nonzero values in the off-diagonal blocks.

### 7.2. Space Charge Impulses

In the previous subsection we saw that, barring space charge, the transfer matrix for each element can be used to propagate a particle's state through the element. In the following subsections we find that the same transfer matrix can also be used to propagate the moments of the beam distribution through the element. Consequently, we would like to formulate a transfer matrix representation for space charge effects. Here we develop such a matrix.

A straightforward approximation that simulates the action of space charge is to "kick" the beam at regular intervals. Specifically, we apply the space charge effect through a section of length $\Delta s$ all at once, as a momentum impulse. This technique is equivalent to modeling space charge as a defocusing thin lens. Of course to maintain accuracy is it necessary that $\Delta s$ be sufficiently small. The magnitude of the impulse is determined by returning to the Newton's inertia equation

(149) $\frac{dp_\alpha}{dt} = F_{s,\alpha} \qquad \alpha \in \{x, y, z\}$,

where $p_\alpha$ is the momentum component in the $\alpha$ direction and $F_{s,\alpha}$ is the self force in the $\alpha$ direction. To illustrate the computation we consider specifically the $x$ phase plane. We start with the expression for the force on a beam particle given by Eqs. (15), considering only the term specific to the self force. Approximating the derivative $dp/dt$ by finite the differences $\Delta p/\Delta t$ and using the linearized electric field of Eq. (71) transforms the above equation into the following approximation:

(150) $\Delta p_x \approx \frac{q}{\gamma^2} E_x \Delta t \approx \frac{q}{\gamma^2} \frac{\langle x E_x \rangle}{\langle x^2 \rangle - \langle x \rangle^2} (x - \bar{x}) \Delta t$.

Recognizing that $\Delta t = \Delta s/v$ and converting to our normalized momentum $x' \equiv p_x/p$ we have

$$\Delta x' \approx \frac{1}{\gamma^2\beta^2}\frac{q}{\gamma mc^2}\frac{\langle xE_x\rangle}{\langle x^2\rangle-\langle x\rangle^2}\Delta s\,(x-\bar{x}),$$
$$= \frac{\Delta s}{f_{sc,x}}\left(x-\langle x\rangle\right), \tag{151}$$

where the thin lens defocal length due to space charge $f_{sc,x}$ (in the $x$ phase plane) is defined as

$$f_{sc,x} \equiv \gamma^3\beta^2\frac{mc^2}{q}\frac{\langle x^2\rangle-\langle x\rangle^2}{\langle xE_x\rangle}. \tag{152}$$

Thus, the action of space charge in the $x$ plane can be written in transfer matrix form, using homogeneous coordinates we have

$$\begin{pmatrix} x_{n+1} \\ x'_{n+1} \\ 1 \end{pmatrix} = \begin{pmatrix} 1 & 0 & 0 \\ \dfrac{\Delta s}{f_{sc,x}} & 1 & -\dfrac{\langle x\rangle\Delta s}{f_{sc,x}} \\ 0 & 0 & 1 \end{pmatrix}\begin{pmatrix} x_n \\ x'_n \\ 1 \end{pmatrix}, \tag{153}$$

where $\Delta s$ is the length over which the space charge effects are being applied.

In the $z$ phase plane the calculations are somewhat different although the result is the same. There the self-force on a particle is $F_{s,z}=qE_z$, however $\Delta z'=(1/\gamma^2)\Delta(\Delta p/p)$ so we end up with the same factor of $\gamma$ in the force terms in all planes. The full transfer matrix $\mathbf{\Phi_{sc}}$ that applies the space charge kick over a distance $\Delta s$ is then

$$\mathbf{\Phi_{sc}} = \begin{pmatrix} 1 & 0 & 0 & 0 & 0 & 0 & 0 \\ \Delta s/f_{sc,x} & 1 & 0 & 0 & 0 & 0 & -\bar{x}\Delta s/f_{sc,x} \\ 0 & 0 & 1 & 0 & 0 & 0 & 0 \\ 0 & 0 & \Delta s/f_{sc,y} & 1 & 0 & 0 & -\bar{y}\Delta s/f_{sc,y} \\ 0 & 0 & 0 & 0 & 1 & 0 & 0 \\ 0 & 0 & 0 & 0 & \Delta s/f_{sc,z} & 1 & -\bar{z}\Delta s/f_{sc,z} \\ 0 & 0 & 0 & 0 & 0 & 0 & 1 \end{pmatrix}. \tag{154}$$

Since $f_{sc,x}$ depends upon $\langle x\rangle$, $\langle x^2\rangle$, and $\langle xE_x\rangle$, these quantities must be recalculated whenever the dimensions of the beam bunch change appreciably. Likewise for the other defocusing strengths $f_{sc,y}$ and $f_{sc,z}$. Specifically we are saying that the space charge transfer matrix is a function of the covariance matrix as well as the distance $\Delta s$, that is,

$$\mathbf{\Phi_{sc}} = \mathbf{\Phi_{sc}}(\boldsymbol{\chi}, \Delta s). \tag{155}$$

Although we are still using matrices to describe the effects of space charge, the result is nonlinear. Consequently, we must be careful when using this technique. The distance $\Delta s$ must be small enough so the above matrix accurately represents the space charge forces through the interval.

### 7.3. Space Charge Defocal Lengths

The values of the space charge defocal lengths can be computed using the results of Section 5.4. There we determined the values of $\langle xE_x\rangle$, $\langle yE_y\rangle$, and $\langle zE_z\rangle$ for an ellipsoidal density distribution analytically, in terms of elliptic integrals. Recall, however, that to simplify the calculations we picked an orthogonal coordinate system centered on the beam centroid and aligned the beam ellipsoid axes. To use these analytic results it is necessary to rotate an arbitrarily oriented ellipsoid into this special coordinate system.

Rather than center the beam on the coordinate origin we may instead compute the moments $\langle (x-\bar{x})E_x \rangle, \langle (y-\bar{y})E_y \rangle$, and $\langle (z-\bar{z})E_z \rangle$. Note, however, that

$$\begin{aligned} \langle (x-\bar{x})E_x \rangle &= \langle xE_x \rangle - \bar{x}\langle E_x \rangle, \\ &= \langle xE_x \rangle, \end{aligned} \tag{156}$$

Since $\langle E_x \rangle$=0 by Newton's third law. The same is true for the moments $\langle yE_y \rangle$ and $\langle zE_z \rangle$ in the other two phase planes. Thus, so long as we use rms envelope values $\sigma_x$, $\sigma_y$, $\sigma_z$ defined in Eqs. (35) in lieu of the moments $\langle x^2 \rangle$, $\langle y^2 \rangle$, $\langle z^2 \rangle$ we can use the expressions for $\langle xE_x \rangle$, $\langle yE_y \rangle$, and $\langle zE_z \rangle$ in Eqs. (113). That is, after we rotate into the proper coordinate system. Recall from Table 1 we see the distribution parameter $\Lambda$ is only loosely coupled to the actual distribution profile. Since $\Lambda$ appears as a factor in the expressions for $\langle xE_x \rangle$, $\langle yE_y \rangle$, and $\langle zE_z \rangle$ in Eqs. (113) we must pick a particular distribution profile for computational purposes. When we supply the value of for the equivalent uniform beam, $\Lambda=2(3/5)^{3/2}$, we find the thin lens defocal lengths to be

$$\begin{aligned} \frac{1}{f_{sc,x}} &= \frac{K}{2}\left[\frac{1}{5\sigma_x^2}\right]^{3/2} R_D\left[\frac{\sigma_y^2}{\sigma_x^2}, \frac{\sigma_z^2}{\sigma_x^2}, 1\right], \\ \frac{1}{f_{sc,y}} &= \frac{K}{2}\left[\frac{1}{5\sigma_y^2}\right]^{3/2} R_D\left[\frac{\sigma_z^2}{\sigma_y^2}, \frac{\sigma_x^2}{\sigma_y^2}, 1\right], \\ \frac{1}{f_{sc,z}} &= \frac{K}{2}\left[\frac{1}{5\sigma_z^2}\right]^{3/2} R_D\left[\frac{\sigma_x^2}{\sigma_z^2}, \frac{\sigma_y^2}{\sigma_z^2}, 1\right], \end{aligned} \tag{157}$$

where $K$ is the beam perveance defined by Eq. (18) and the $\sigma_x$, $\sigma_y$, $\sigma_z$ are the rms envelopes defined in Eqs. (35). The above values are the defocal lengths for an ellipsoid that is centered and aligned to the beam axes.

To rotate our beam ellipsoid into its natural coordinate system consider the following matrix composed of elements of the covariance matrix $\boldsymbol{\sigma}$:

$$\boldsymbol{\tau} \equiv \begin{pmatrix} \langle x^2 \rangle & \langle xy \rangle & \langle xz \rangle \\ \langle xy \rangle & \langle y^2 \rangle & \langle yz \rangle \\ \langle xz \rangle & \langle yz \rangle & \langle z^2 \rangle \end{pmatrix}. \tag{158}$$

The off-diagonal terms $\langle xy \rangle$, $\langle xz \rangle$, $\langle yz \rangle$ of $\boldsymbol{\tau}$ indicate coupling between the phase planes. Note that $\boldsymbol{\tau}$ is positive definite and symmetric, therefore it is diagonalizable having a complete set of orthonormal eigenvectors. Consequently we can find a matrix $\mathbf{R}$ in the special orthogonal group $SO(3)$ that diagonalizes $\boldsymbol{\tau}$. That is,

$$\boldsymbol{\tau} = \mathbf{R}\,\mathbf{D}\,\mathbf{R}^T, \tag{159}$$

where $\mathbf{D}$ is the diagonal matrix of eigenvalues of $\boldsymbol{\tau}$. If the set orthonormal (column) eigenvectors of $\boldsymbol{\tau}$ is $\{\mathbf{e}_1,\mathbf{e}_2,\mathbf{e}_3\}$ then the matrix $\mathbf{R}$ is composed as follows:

$$\mathbf{R} = \begin{pmatrix} r_{11} & r_{12} & r_{13} \\ r_{21} & r_{22} & r_{23} \\ r_{31} & r_{32} & r_{33} \end{pmatrix} = \left(\mathbf{e}_1 \vdots \mathbf{e}_2 \vdots \mathbf{e}_3\right). \tag{160}$$

The fact that the set $\{\mathbf{e}_1,\mathbf{e}_2,\mathbf{e}_3\}$ is orthonormal insures that $\mathbf{R}$ is a member of the special orthogonal group $SO(3)$.

From Section 5.2 we see that the matrix **R** is exactly the rotation that aligns the ellipsoid axes to the coordinate system. The extension to full six-dimensional phase space rotation is straightforward. Because of the Euclidean nature of $\Re^6$ the tangent planes corresponding to the momentum space ($x'$,$y'$,$z'$) get rotated by the same angle and axis as does the configuration space ($x$,$y$,$z$). This action in homogeneous coordinates is continues through since there is no translation. Consequently, the proper rotation **R** in homogeneous phase space coordinates $\mathbf{z}=(x,x',y,y',z,z',1)$ is given by

$$\mathbf{R} = \begin{pmatrix} r_{11} & 0 & r_{12} & 0 & r_{13} & 0 & 0 \\ 0 & r_{11} & 0 & r_{12} & 0 & r_{13} & 0 \\ r_{21} & 0 & r_{22} & 0 & r_{23} & 0 & 0 \\ 0 & r_{21} & 0 & r_{22} & 0 & r_{23} & 0 \\ r_{31} & 0 & r_{32} & 0 & r_{33} & 0 & 0 \\ 0 & r_{31} & 0 & r_{32} & 0 & r_{33} & 0 \\ 0 & 0 & 0 & 0 & 0 & 0 & 1 \end{pmatrix}. \tag{161}$$

The proper space charge kick for an ellipsoid in general position is found by rotating phase space by **R**, applying the momentum in the aligned coordinates, then rotating back by $\mathbf{R}^T$. Thus, if we replace the transfer matrix $\mathbf{\Phi}_{sc}$ with $\mathbf{R}^T\mathbf{\Phi}_{sc}\mathbf{R}$ we can treat arbitrarily oriented beam ellipsoids.

### 7.4. Equations for Centroid Motion

We find the equations that propagate the mean value vector simply by taking the moment of Eq. (147) for the full phase coordinate vector $\mathbf{z_n}$. Since the transfer matrix $\mathbf{\Phi_n}$ does not depend upon the phase space coordinates, we get

$$\left\langle \mathbf{z_{n+1}} \right\rangle = \mathbf{\Phi_n} \left\langle \mathbf{z_n} \right\rangle, \tag{162}$$

or

$$\bar{\mathbf{z}}_{\mathbf{n+1}} = \mathbf{\Phi_n} \bar{\mathbf{z}}_{\mathbf{n}}, \tag{163}$$

where

$$\bar{\mathbf{z}}_{\mathbf{n}} \equiv \bar{\mathbf{z}}(s_n), \tag{164}$$

the value $s_n$ being the location of the entrance to the $n^{\text{th}}$ beamline element. Recall that there are no space charge effects for centroid motion. Therefore, we do not apply any space charge kicks when propagating these moments. We simply multiply $\bar{\mathbf{z}}_{\mathbf{n}}$ by the transfer matrix $\mathbf{\Phi_n}$ for each element $n$ in the beam line.

### 7.5. Equations for the Second-Order Moments

For simplicity, once again consider only the $x$ phase plane. The continuous evolution equation for $\boldsymbol{\sigma}_{\mathbf{xx}}$ can be found by direct differentiation of $\boldsymbol{\sigma}_{\mathbf{xx}}$ with respect to $s$, then applying Liouville's theorem and Eq. (141). From the definition of $\boldsymbol{\sigma}_{\mathbf{xx}}$ we find

$$\begin{aligned} \boldsymbol{\sigma}_{\mathbf{xx}}' &= \left\langle \mathbf{x}'\mathbf{x}^{\mathbf{T}} \right\rangle + \left\langle \mathbf{x}\mathbf{x}'^{\mathbf{T}} \right\rangle \\ &= \mathbf{A}\left\langle \mathbf{x}\mathbf{x}^{\mathbf{T}} \right\rangle + \left\langle \mathbf{x}\mathbf{x}^{\mathbf{T}} \right\rangle \mathbf{A}^{\mathbf{T}} \\ &= \mathbf{A}\boldsymbol{\sigma}_{\mathbf{xx}} + \boldsymbol{\sigma}_{\mathbf{xx}}\mathbf{A}^{\mathbf{T}} \end{aligned} \tag{165}$$

The solution to this matrix differential equation is given (formally) by

$$\boldsymbol{\sigma}_{\mathbf{xx}}(s) = \mathbf{\Phi}(s)\boldsymbol{\sigma}_{\mathbf{xx}}(0)\mathbf{\Phi}^{\mathbf{T}}(s), \tag{166}$$

where $\mathbf{\Phi}(s)$ is the fundamental matrix solution of Eq. (144), and $\boldsymbol{\sigma}_{\mathbf{xx}}(0)$ is the initial covariance matrix for the $x$ plane. (This fact may be checked by direct differentiation.) The above equation also holds for the

entire set of second moment $\boldsymbol{\sigma}$ when using the fully augmented fundamental matrix $\boldsymbol{\Phi}(s)$. Recalling that the transfer matrix for an element is found by evaluating the fundamental matrix at the end of the element (i.e., $\boldsymbol{\Phi}_n=\boldsymbol{\Phi}(l_n)$, where $l_n$ is the length of the $n^{th}$ element) leads to the following transfer equation for the second-order moments:

$$\boldsymbol{\sigma}_{n+1} = \boldsymbol{\Phi}_n \boldsymbol{\sigma}_n \boldsymbol{\Phi}_n^T, \tag{167}$$

where

$$\boldsymbol{\sigma}_n \equiv \boldsymbol{\sigma}(s_n). \tag{168}$$

We see that advancing the state of the second-order moments through the $n^{th}$ beamline element is accomplished by transpose conjugation of $\boldsymbol{\sigma}$ with the transfer matrix $\boldsymbol{\Phi}_n$. However, we must still include the effects of space charge.

Space charge effects are imposed using a transfer equation analogous to (167). However, here we conjugate $\boldsymbol{\sigma}$ with the space charge transfer matrix $\boldsymbol{\Phi}_{sc}$. Recall that the space charge transfer matrix $\boldsymbol{\Phi}_{sc}$ is a function of the covariance matrix $\boldsymbol{\sigma}$. Therefore, for accurate simulation of long beamline elements it may be necessary to split the beamline element into several subsections, applying the space charge kick after each subsection. Specifically, we advance $\boldsymbol{\sigma}$ by the transfer matrix for a subsection, conjugate by $\boldsymbol{\Phi}_{sc}$, and repeat until we are through the element.

### 7.6. Extensions to the Inhomogeneous Case

In some particle beam situations the modeling equations are inhomogeneous, that is, they contain a forcing term. For beamline elements, this is the case for dipole magnets, for example when used as beam steering magnets (for example, see Appendix A.3 ). Many control systems also have modeling equations of this type. Let the transfer equations for an inhomogeneous element be given as

$$\mathbf{z}_{n+1} = \boldsymbol{\Phi}_n \mathbf{z}_n + \boldsymbol{\Gamma}_n \mathbf{u}_n \tag{169}$$

where $\mathbf{z}_n$ is the 6×1 column vector of phase space coordinates, $\boldsymbol{\Phi}_n$ is the 6×6 transfer matrix, $\boldsymbol{\Gamma}_n$ is a 6x$M$ matrix, and $\mathbf{u}_n$ is a column vector of length $M$. Note that this is still a linear system (in $\mathbf{z}_n$ and $\mathbf{u}_n$) only now we have a forcing term driven by $\mathbf{u}_n$. The vector $\mathbf{u}_n$ represents some external parameters for the element, perhaps a control parameter or perhaps an unknown noise source (in this case $\mathbf{u}_n$ would be a random variable).

We can compute the propagation equations for $\boldsymbol{\sigma}_n$ simply by unwinding the definition and using the above transfer equation. We get

$$\begin{aligned} \boldsymbol{\sigma}_{n+1} &= \left\langle \mathbf{z}_{n+1} \mathbf{z}_{n+1}^T \right\rangle, \\ &= \left\langle (\boldsymbol{\Phi}_n \mathbf{z}_n + \boldsymbol{\Gamma}_n \mathbf{u}_n)(\boldsymbol{\Phi}_n \mathbf{z}_n + \boldsymbol{\Gamma}_n \mathbf{u}_n)^T \right\rangle, \\ &= \boldsymbol{\Phi}_n \boldsymbol{\sigma}_n \boldsymbol{\Phi}_n^T + \boldsymbol{\Phi}_n \mathbf{X}_n \boldsymbol{\Gamma}_n^T + \boldsymbol{\Gamma}_n \mathbf{X}_n^T \boldsymbol{\Phi}_n^T + \boldsymbol{\Gamma}_n \mathbf{Y}_n \boldsymbol{\Gamma}_n^T, \end{aligned} \tag{170}$$

where

$$\begin{aligned} \mathbf{X}_n &\equiv \left\langle \mathbf{z}_n \mathbf{u}_n^T \right\rangle, \\ \mathbf{Y}_n &\equiv \left\langle \mathbf{u}_n \mathbf{u}_n^T \right\rangle. \end{aligned} \tag{171}$$

The 6×$M$ matrix $\mathbf{X}_n$ is the cross-correlation matrix between the phase-space coordinates and the input vector. The $M$×$M$ symmetric matrix $\mathbf{Y}_n$ is the covariance matrix of the drive vector. Note that if $\mathbf{u}_n$ is a scalar value, say $u_n$, then $\mathbf{X}_n = u_n \bar{\mathbf{z}}$ and $\mathbf{Y}_n = u_n^2$.

The matrix $\boldsymbol{\Gamma}_n$ is given by the structure of the system, representing coupling between the particle state and the external drive source $\mathbf{u}_n$. Thus, to use the above transfer equations for $\boldsymbol{\sigma}_n$ it is necessary to determine $\mathbf{X}_n$ and $\mathbf{Y}_n$. Typically $\mathbf{X}_n$ is zero, it represents the correlation between the drive vector $\mathbf{u}_n$ and the

coordinates in phase space **z**. Most systems are designed to avoid any such correlations. When $\mathbf{u_n}$ is a random variable (representing noise or other unknown), the matrix $\mathbf{Y_n}$ is the autocorrelation. For most systems it can be determined, at least approximately, through measurement. When $\mathbf{u_n}$ is deterministic, $\mathbf{Y_n}$ is essentially just $\mathbf{u_n}$ squared, which is easily determined.

### 7.7. Homogeneous Coordinates

Here we again consider inhomogeneous systems, however, now we assume the special form

$$\mathbf{z_{n+1}} = \mathbf{\Phi_n z_n} + \mathbf{u_n}\,, \tag{172}$$

where $\mathbf{u_n} \in \Re^6$ is the external drive vector. That is, the external driving forces can be described as a vector in phase space. This situation occurs when the effects of an inhomogeneous element behave as translations in phase space, such as those produced by an ideal dipole magnet. In this situation we can form a convenient augmented state variable system that has the same form as the homogeneous transfer equations.

Mathematicians typically use homogeneous coordinates to parameterize the projective spaces $P^n$. They are also widely used in computer graphics for three-dimensional rendering, since translation, rotation, and scaling can all be performed by matrix multiplication [20]. The $n$-dimensional real projective space $\Re P^n$ can be described as a set equivalence relations $[x_0, \ldots, x_n]$ on $\Re^{n+1}$ where $[x_0, \ldots, x_n] \sim [wx_0, \ldots, wx_n]$ for all real $w \neq 0$, and such that not all the $x_i$ are zero. Thus, the points of the project space $\Re P^n$ are seen to be the lines in $\Re^{n+1}$ that pass through the origin. These equivalence classes are known as the homogeneous coordinates of the projective spaces. (Another equivalent description of the projective space $\Re P^n$ is found by identifying all the antipodal points of the sphere $S^n$.) The projective space $\Re P^n$ can be considered a differentiable manifold with the atlas consisting of $n+1$ charts $\{U_i, \phi_i\}_{i=0}^{\ n}$ where $U_i$ is the set of equivalence relations $[x_0, \ldots, x_n]$ such that $x_i \neq 0$, and $\phi_i : U_i \to \Re^n$ is the bijective coordinate map

$$\phi_i : [x_0, \ldots, x_i, \ldots x_n] \mapsto (x_0 / x_i, \ldots, \hat{x}_i, \ldots x_n / x_i)\,. \tag{173}$$

The caret indicates omission of the coordinate. Note that the union $\cup_{i=0}^{\ n} U_i$ covers all of $\Re P^n$. More aptly, note that the coordinates of the $n+1$ chart consist of the following equivalence relations:

$$\phi_i^{-1}(x_0, \ldots, x_{n-1}) = [x_0, \ldots x_{n-1}, 1] \quad \forall (x_0, \ldots x_{n-1}) \in \Re^n\,. \tag{174}$$

Thus, $U_i$ is seen to be the set of all lines in $\Re^{n+1}$ passing through the plane $\{(x_0, \ldots, x_n) \in \Re^{n+1} \,|\, x_n = 1\}$. We shall use the homogeneous coordinates of this chart.

Let the augmented phase space coordinate $\boldsymbol{\zeta}$ be

$$\boldsymbol{\zeta} \equiv \begin{bmatrix} \mathbf{z} \\ 1 \end{bmatrix} = \begin{pmatrix} x & x' & y & y' & z & z' & 1 \end{pmatrix}^T\,. \tag{175}$$

Then system (172) can be written in the form

$$\boldsymbol{\zeta}_{\mathbf{n+1}} = \mathbf{\Theta_n} \boldsymbol{\zeta}_{\mathbf{n}}\,, \tag{176}$$

where the 7×7 matrix $\boldsymbol{\theta}_{\mathbf{n}}$ is defined as the augmented square matrix

$$\mathbf{\Theta_n} = \begin{bmatrix} \mathbf{\Phi_n} & \mathbf{u_n} \\ \mathbf{0} & 1 \end{bmatrix}. \tag{177}$$

This is exactly the form of the homogeneous transfer equations. Therefore, if we only encounter inhomogeneous transfer systems of the special form given above, by employing homogeneous coordinates we can convert back to homogeneous transfer equations.

For envelope calculations consider the modified covariance matrix $\boldsymbol{\tau}$ formed from the phase space vector $\boldsymbol{\zeta}$ according to

$$\boldsymbol{\tau} \equiv \left\langle \boldsymbol{\zeta} \boldsymbol{\zeta}^T \right\rangle. \tag{178}$$

To simplify the discussion, consider only the *x*-plane phase space. In the homogeneous coordinates the *x*-plane phase coordinates are given by

$$\xi \equiv \begin{bmatrix} \mathbf{x} \\ 1 \end{bmatrix} = \begin{pmatrix} x & x' & 1 \end{pmatrix}^T . \tag{179}$$

Thus, the modified *x*-plane correlation matrix $\boldsymbol{\tau}_{\mathbf{xx}}$ is formed by

$$\boldsymbol{\tau}_{\mathbf{xx}} \equiv \left\langle \xi\xi^T \right\rangle = \begin{pmatrix} \langle x^2 \rangle & \langle xx' \rangle & \langle x \rangle \\ \langle xx' \rangle & \langle x'^2 \rangle & \langle x' \rangle \\ \langle x \rangle & \langle x' \rangle & 1 \end{pmatrix} = \begin{bmatrix} \boldsymbol{\sigma}_{\mathbf{xx}} & \bar{\mathbf{x}} \\ \bar{\mathbf{x}}^T & 1 \end{bmatrix}. \tag{180}$$

We see that in the homogeneous phase space coordinates the covariance matrix $\boldsymbol{\tau}$ contains the original covariance matrix $\boldsymbol{\sigma}$ plus the mean value vector $\bar{\mathbf{z}}$. Moreover, transpose conjugation of the covariance matrix $\boldsymbol{\tau}_{\mathbf{xx}}$ by the transfer matrix $\boldsymbol{\Theta}_{\mathbf{n}}$ yields the following augmented system:

$$\boldsymbol{\tau}_{\mathbf{n+1}} = \boldsymbol{\Theta}_{\mathbf{n}} \boldsymbol{\tau}_{\mathbf{n}} \boldsymbol{\Theta}_{\mathbf{n}}{}^T = \begin{bmatrix} \boldsymbol{\Phi}_{\mathbf{n}} \boldsymbol{\sigma}_{\mathbf{n}} \boldsymbol{\Phi}_{\mathbf{n}}{}^T + \boldsymbol{\Phi}_{\mathbf{n}} \bar{\mathbf{z}} \mathbf{u}^T + \mathbf{u} \bar{\mathbf{z}}^T \boldsymbol{\Phi}_{\mathbf{n}}{}^T + \mathbf{u}\mathbf{u}^T & \boldsymbol{\Phi}_{\mathbf{n}} \bar{\mathbf{z}}_{\mathbf{n}} + \mathbf{u}_{\mathbf{n}} \\ \bar{\mathbf{z}}_{\mathbf{n}}{}^T \boldsymbol{\Phi}_{\mathbf{n}}{}^T + \mathbf{u}_{\mathbf{n}}{}^T & 1 \end{bmatrix}. \tag{181}$$

The upper left block is exactly the covariance transfer equation for the inhomogeneous system (172). The diagonal blocks are the transfer equation, and its transpose, for the mean value vector. Consequently, both the transfer equation for the mean value evolution and the covariance evolution are included in the modified transfer system.

To make the use of homogeneous coordinates more explicit, consider the case of an ideal dipole-correcting magnet in the *x* phase plane. The effect of such a device is to add an impulsive kick in the particle momentum of intensity $\Delta x'$. Thus, the modified transfer matrix for the *x* phase plane would appear as

$$\boldsymbol{\Theta}_{\mathbf{dipole}} = \begin{pmatrix} 1 & 0 & 0 \\ 0 & 1 & \Delta x' \\ 0 & 0 & 1 \end{pmatrix}. \tag{182}$$

The effects of the ideal dipole are found by transpose conjugation of the modified covariance matrix $\boldsymbol{\tau}_{\mathbf{xx}}$ by the above transfer matrix; we have

$$\begin{aligned} \boldsymbol{\Theta}_{\mathbf{dipole}} \boldsymbol{\tau}_{\mathbf{xx}} \boldsymbol{\Theta}_{\mathbf{dipole}}{}^T &= \begin{pmatrix} 1 & 0 & 0 \\ 0 & 1 & \Delta x' \\ 0 & 0 & 1 \end{pmatrix} \begin{pmatrix} \langle x^2 \rangle & \langle xx' \rangle & \bar{x} \\ \langle xx' \rangle & \langle x'^2 \rangle & \bar{x}' \\ \bar{x} & \bar{x}' & 1 \end{pmatrix} \begin{pmatrix} 1 & 0 & 0 \\ 0 & 1 & 0 \\ 0 & \Delta x' & 1 \end{pmatrix}, \\ &= \begin{pmatrix} \langle x^2 \rangle & \langle xx' \rangle + \bar{x}\Delta x' & \bar{x} \\ \langle xx' \rangle + \bar{x}\Delta x' & \langle x'^2 \rangle + 2\bar{x}'\Delta x' + \Delta x'^2 & \bar{x}' + \Delta x' \\ \bar{x} & \bar{x}' + \Delta x' & 1 \end{pmatrix}. \end{aligned} \tag{183}$$

We can clearly see the effects of an impulsive kick on the entire beam, both in the centroid behavior and the rms envelope behavior.

## 8. SUMMARY AND CONCLUSION

Beam envelope simulation as described here is a computationally inexpensive way to obtain particle beam behavior to first order. Rather than propagating an ensemble of particles then computing the statistics to determine the rms beam properties, we propagate the rms beam properties directly. We have seen that

theoretically that this is a valid approach. However, there are clearly limitations to simulation results generated in such a manner. The techniques described here are intended to give a quick insight into general beam behavior and not to be used as a tool for detailed dynamics analysis. Consequently the simulation methods here are appropriate for initial off-line design studies and for on-line model reference control applications, where fast real-time response is essential.

The validity off our analysis typically comes into concern because, by practical considerations, we are forced to make some simplifying assumptions to implement the simulation procedures. The first assumption we make is the applicability of Liouville's theorem to form the evolution equations for the distribution's moments. Technically, Liouville's theorem is valid only in $6N$ dimensional phase space for collisionless system, where $N$ is the number of beam particles. However, it is approximately true whenever the collective fields of the beam can be accurately described by smooth functions. Thus, we have assumed that our beam is populous enough, and compact enough for this condition to be true. Another circumstance where this assumption holds is for relatively cold beams. Both situations assume that the Debye length of the beam is small enough so that any particle see mostly collective fields and there are few collision-like encounters. The next critical assumption comes in the form of ellipsoidal symmetry. That is, we assume that the beam exhibits ellipsoidal symmetry in configuration space. Under this assumption we are able to analytically compute the effects of space charge on the moment dynamics. Unfortunately it is known that ellipsoidally symmetric beams are not, in general, stationary beams [24], the only one of this type is the KV, or micro-canonical distribution. Thus, we must assume that our true beam is very close to an ellipsoidal one. Fortunately ellipsoidal beams can accurately represent many laboratory beams.

The last major assumption is that of linearity. Specifically, we assume not only that all external forces are linear, but also that internal forces (i.e., self forces) are linear. Consequently any nonlinear effects from a beamline element cannot be modeled, for example, fringe fields, higher order field components, etc. Our linear model for the internal fields essentially constitutes the assumption of constant rms emittances. This is true for both the rms envelope equations and the transfer matrix method. There is no known practical method for simulating emittance growth using only beam statistics. Currently, only full multiple particle simulations have this capability. However, it is possible to assign emittance growths based on analytic approximations or a priori knowledge of emittance values. In the envelope equations we just assign the emittance values directly, for the transfer matrix approach we multiply the second-order covariant by the growth factor.

## ACKNOWLEDGEMENTS

The author wishes to thank Tom Wangler for many valuable discussions on beam physics and for his time reviewing the manuscript. Nicholas Pattengale was invaluable in designing and prototyping software implementing the simulation techniques described herein.

## APPENDIX A: TRANSFER MATRICES FOR COMMON BEAMLINE ELEMENTS

We describe here the transfer matrices for some beamline elements in common use. As was done with the $\boldsymbol{\sigma}$ matrix, we decompose a general transfer matrix $\boldsymbol{\Phi}$ into 2×2 composite matrices according to the following:

$$\text{(A.1)} \qquad \boldsymbol{\Phi} = \begin{pmatrix} \boldsymbol{\Phi}_{\mathbf{xx}} & \boldsymbol{\Phi}_{\mathbf{xy}} & \boldsymbol{\Phi}_{\mathbf{xz}} \\ \boldsymbol{\Phi}_{\mathbf{yx}} & \boldsymbol{\Phi}_{\mathbf{yy}} & \boldsymbol{\Phi}_{\mathbf{yz}} \\ \boldsymbol{\Phi}_{\mathbf{zx}} & \boldsymbol{\Phi}_{\mathbf{zy}} & \boldsymbol{\Phi}_{\mathbf{zz}} \end{pmatrix}.$$

In most cases only the block diagonal sub-matrices $\boldsymbol{\Phi}_{\mathbf{xx}}$, $\boldsymbol{\Phi}_{\mathbf{yy}}$, and $\boldsymbol{\Phi}_{\mathbf{zz}}$ are nonzero. Nonzero values of the off-diagonal sub-matrices indicate coupling between phase planes.

Many transfer matrices exhibit a semi-group property. Specifically, if we denote the transfer matrix of an element of length $\Delta s$ as $\boldsymbol{\Phi}(\Delta s)$, then the transfer matrix for two such elements is $\boldsymbol{\Phi}(\Delta s)\boldsymbol{\Phi}(\Delta s)$. In general, for arbitrary lengths $\Delta s_1$ and $\Delta s_2$ we have

$$\text{(A.2)} \qquad \boldsymbol{\Phi}(\Delta s_1 + \Delta s_2) = \boldsymbol{\Phi}(\Delta s_1)\boldsymbol{\Phi}(\Delta s_2).$$

### A.1 Drift Space

The transfer matrix $\boldsymbol{\Phi}$ for a drift space of length $\Delta s$ is given in terms of its nonzero diagonal blocks

$$\text{(A.3)} \qquad \boldsymbol{\Phi}_{\mathbf{xx}} = \begin{pmatrix} 1 & \Delta s \\ 0 & 1 \end{pmatrix}, \qquad \boldsymbol{\Phi}_{\mathbf{yy}} = \begin{pmatrix} 1 & \Delta s \\ 0 & 1 \end{pmatrix}, \qquad \boldsymbol{\Phi}_{\mathbf{zz}} = \begin{pmatrix} 1 & \Delta s \\ 0 & 1 \end{pmatrix},$$

where the sub-matrix for the $z$ plane assumes that the coordinates are $(z,z')$. If the coordinates are $(z,\Delta p/p)$ then the sub-matrix is

$$\text{(A.4)} \qquad \boldsymbol{\Phi}_{\mathbf{zz}} = \begin{pmatrix} 1 & \Delta s/\gamma^2 \\ 0 & 1 \end{pmatrix}.$$

This transfer matrix has the semi-group property.

### A.2 Quadrupole

In the case of an ideal quadrupole lens where the forces are linear throughout and the fringe fields are negligible, the transfer matrix block diagonals are

$$\text{(A.5)} \qquad \boldsymbol{\Phi}_{\mathbf{foc}} = \begin{pmatrix} \cos kl & \frac{1}{k}\sin kl \\ -k\sin kl & \cos kl \end{pmatrix}, \qquad \boldsymbol{\Phi}_{\mathbf{def}} = \begin{pmatrix} \cosh kl & \frac{1}{k}\sinh kl \\ k\sinh kl & \cosh kl \end{pmatrix}, \qquad \boldsymbol{\Phi}_{\mathbf{zz}} = \begin{pmatrix} 1 & l \\ 0 & 1 \end{pmatrix},$$

where $\boldsymbol{\Phi}_{\mathbf{foc}}$ represents the block diagonal of the focusing plane and $\boldsymbol{\Phi}_{\mathbf{def}}$ represents the block diagonal of the defocusing plane of the quadrupole. The quantity $l$ is the length of the quadrupole and $k$ is the quadrupole focusing strength, it has the values

$$\text{(A.6)} \qquad \begin{aligned} k_{mag} &= \sqrt{\frac{qG}{\beta\gamma mc}} \\ k_{esq} &= \frac{1`}{\beta a}\sqrt{\frac{qV_0}{\gamma mc^2}} \end{aligned}$$

where $k_{mag}$ is the value for a magnetic quadrupole and $k_{esq}$ is the value for an electrostatic quadrupole. Here $G$ is the magnetic field gradient at the beam axis, $V_0$ is the electrostatic electrode potential and $a$ is the aperture of the quadrupole.

### A.3 Dipole Steering Magnet (As a Thin Lens)

We may treat a dipole magnet as a thin lens by again approximating the time derivative of momentum as a finite difference in the equations of motion. The equation of motion for a particle in a dipole field of strength **B** is

$$\begin{aligned}\frac{d\mathbf{p}}{dt} &= q\mathbf{v}\times\mathbf{B}\,,\\ &= q\beta c(x',y',1+z')\times(B_x,B_y,0)\,,\end{aligned} \tag{A.7}$$

where we have assumed the magnetic field is constant throughout the magnet. Approximating the derivative by a finite difference gives us the equations

$$\begin{aligned}\Delta p_x &= -q(1+z')B_y\Delta s\,,\\ \Delta p_y &= q(1+z')B_x\Delta s\,,\\ \Delta p_z &= q(x'B_y - y'B_x)\Delta s\,,\end{aligned} \tag{A.8}$$

Using the relations $\Delta x'=\Delta p_x/p$, $\Delta y'=\Delta p_y/p$, $\Delta z'=(1/\gamma^2)\Delta p_z/p$, we can form the transfer system

$$\begin{pmatrix} x_{n+1}\\ x'_{n+1}\\ y_{n+1}\\ y'_{n+1}\\ z_{n+1}\\ z'_{n+1}\end{pmatrix} = \begin{pmatrix} 1 & 0 & 0 & 0 & 0 & 0\\ 0 & 1 & 0 & 0 & 0 & \omega_x\Delta s\\ 0 & 0 & 1 & 0 & 0 & 0\\ 0 & 0 & 0 & 1 & 0 & \omega_y\Delta s\\ 0 & 0 & 0 & 0 & 1 & 0\\ 0 & \omega_x\Delta s/\gamma^2 & 0 & \omega_y\Delta s/\gamma^2 & 0 & 1\end{pmatrix}\begin{pmatrix} x_n\\ x'_n\\ y_n\\ y'_n\\ z_n\\ z'_n\end{pmatrix} + \begin{pmatrix} 0\\ \omega_x\Delta s\\ 0\\ \omega_y\Delta s\\ 0\\ 0\end{pmatrix}, \tag{A.9}$$

where

$$\omega_x \equiv -\frac{qB_y}{\beta\gamma mc} \qquad \text{and} \qquad \omega_y \equiv \frac{qB_x}{\beta\gamma mc} \tag{A.10}$$

are the cyclotron phase advances in the $x$ and $y$ directions respectively.

Since the contributions from the phase space coordinates are usually small we can often approximate the dipole effect using only the additive term in the above. Referring to Section 7.6, in this case we have $\boldsymbol{\Gamma}=\mathbf{I}$ and

$$\mathbf{X} = \begin{pmatrix} 0 & \bar{x}\omega_x & 0 & \bar{x}\omega_y & 0 & 0\\ 0 & \overline{x'}\omega_x & 0 & \overline{x'}\omega_y & 0 & 0\\ 0 & \bar{y}\omega_x & 0 & \bar{y}\omega_y & 0 & 0\\ 0 & \overline{y'}\omega_x & 0 & \overline{y'}\omega_y & 0 & 0\\ 0 & \bar{z}\omega_x & 0 & \bar{z}\omega_y & 0 & 0\\ 0 & \overline{z'}\omega_x & 0 & \bar{z}\omega_y & 0 & 0\end{pmatrix}, \quad \mathbf{Y} = \begin{pmatrix} 0 & 0 & 0 & 0 & 0 & 0\\ 0 & \omega_x^2 & 0 & \omega_x\omega_y & 0 & 0\\ 0 & 0 & 0 & 0 & 0 & 0\\ 0 & \omega_x\omega_y & 0 & \omega_y^2 & 0 & 0\\ 0 & 0 & 0 & 0 & 0 & 0\\ 0 & 0 & 0 & 0 & 0 & 0\end{pmatrix}. \tag{A.11}$$

### A.4 Thick Dipole Magnet

A thick dipole magnet can be used for beam bending as well as steering. Here we present the full solutions for particle trajectories through constant magnetic fields oriented in the transverse directions. These solutions can be computed analytically and put into transfer matrix form. From the full solutions one can derive transfer matrices for dipole magnets having fields directed in only one plane. Starting from the Lorentz forces the differential equations describing the motion are

$$
\begin{aligned}
x'' &= -\omega_x\left(1+z'\right), \\
y'' &= -\omega_y\left(1+z'\right), \\
z'' &= \omega_x x' + \omega_y y',
\end{aligned}
\tag{A.12}
$$

where

$$
\omega_x \equiv -\frac{qB_y}{\beta\gamma mc} \qquad \text{and} \qquad \omega_y \equiv \frac{qB_x}{\beta\gamma mc}
\tag{A.13}
$$

are the cyclotron frequencies in the $x$ and $y$ directions. The above equations can be solved to give us the transfer matrix

$$
\mathbf{\Phi} = \begin{pmatrix}
1 & \left(\frac{\omega_x^2}{\omega_c^3}\sin\omega_c\Delta s + \frac{\omega_y^2}{\omega_c^2}\Delta s\right) & 0 & \frac{\omega_x\omega_y}{\omega_c^3}\left(\sin\omega_c\Delta s - \omega_c\Delta s\right) & 0 & \frac{\omega_x}{\omega_c^2}\left(\cos\omega_c\Delta s - 1\right) \\
0 & \left(\frac{\omega_x^2}{\omega_c^2}\cos\omega_c\Delta s + \frac{\omega_y^2}{\omega_c^2}\right) & 0 & \frac{\omega_x\omega_y}{\omega_c^2}\left(\cos\omega_c\Delta s - 1\right) & 0 & \frac{\omega_x}{\omega_c}\sin\omega_c\Delta s \\
0 & \frac{\omega_x\omega_y}{\omega_c^3}\left(\sin\omega_c\Delta s - \omega_c\Delta s\right) & 1 & \left(\frac{\omega_y^2}{\omega_c^3}\sin\omega_c\Delta s + \frac{\omega_x^2}{\omega_c^2}\Delta s\right) & 0 & \frac{\omega_y}{\omega_c^2}\left(\cos\omega_c\Delta s - 1\right) \\
0 & \frac{\omega_x\omega_y}{\omega_c^2}\left(\cos\omega_c\Delta s - 1\right) & 0 & \left(\frac{\omega_y^2}{\omega_c^2}\cos\omega_c\Delta s + \frac{\omega_x^2}{\omega_c^2}\right) & 0 & \frac{\omega_y}{\omega_c}\sin\omega_c\Delta s \\
0 & \frac{\omega_x}{\omega_c^2}\left(\cos\omega_c\Delta s - 1\right) & 0 & \frac{\omega_y}{\omega_c^2}\left(\cos\omega_c\Delta s - 1\right) & 1 & \frac{\sin\omega_c\Delta s}{\omega_c} \\
0 & \frac{\omega_x}{\omega_c}\sin\omega_c\Delta s & 0 & \frac{\omega_y}{\omega_c}\sin\omega_c\Delta s & 0 & \cos\omega_c\Delta s
\end{pmatrix},
\tag{A.14}
$$

and drive vector

$$
\mathbf{u} = \begin{pmatrix}
\frac{\omega_x}{\omega_c^2}\left(\cos\omega_c\Delta s - 1\right) \\
\frac{\omega_x}{\omega_c}\sin\omega_c\Delta s \\
\frac{\omega_y}{\omega_c^2}\left(\cos\omega_c\Delta s - 1\right) \\
\frac{\omega_y}{\omega_c}\sin\omega_c\Delta s \\
\frac{\sin\omega_c\Delta s}{\omega_c} - \Delta s \\
\cos\omega_c\Delta s - 1
\end{pmatrix},
\tag{A.15}
$$

where

$$
\omega_c = \sqrt{\omega_x^2 + \omega_y^2}\ .
\tag{A.16}
$$

Note that again $\mathbf{\Gamma}=\mathbf{I}$. Note also that in the limit as $\Delta s \to 0$ the transfer matrix and drive vector approach the thin lens approximation but with the drift component.

$$\text{(A.17)}\quad \lim_{\Delta s\to\infty}\mathbf{\Phi}=\begin{pmatrix}1 & \Delta s & 0 & 0 & 0 & 0\\ 0 & 1 & 0 & 0 & 0 & \omega_x\Delta s\\ 0 & 0 & 1 & \Delta s & 0 & 0\\ 0 & 0 & 0 & 1 & 0 & \omega_y\Delta s\\ 0 & 0 & 0 & 0 & 1 & \Delta s\\ 0 & \omega_x\Delta s & 0 & \omega_y\Delta s & 0 & 1\end{pmatrix},\qquad \lim_{\Delta s\to\infty}\mathbf{u}=\begin{pmatrix}0\\ \omega_x\Delta s\\ 0\\ \omega_y\Delta s\\ 0\\ 0\end{pmatrix}.$$

### A.5 Sector Bending Magnet

In a sector bending magnet the design trajectory is where the force from centripetal acceleration exactly balances the magnetic force, it is an arc with radius $R_0$. To analyze a bending magnet we usually employ a perturbational analysis around the design trajectory in cylindrical coordinates $(r,\theta,z)$. Figure 6 demonstrates how we construct the beam coordinates $(x,y,z)$ as perturbations around the synchronous trajectory of $r=R_0$.

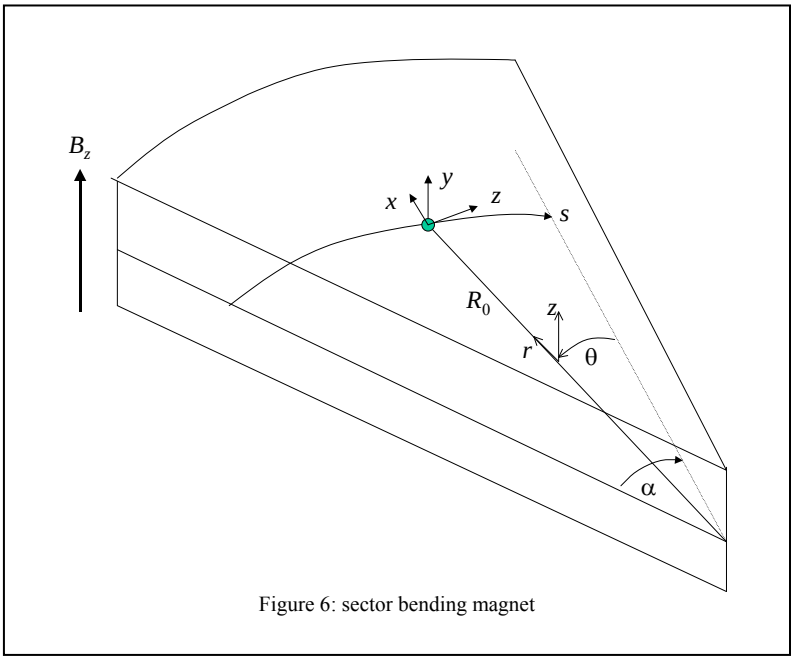

Figure 6: sector bending magnet

Clearly the bend angle $\alpha$ is a parameter of the bending magnet. The radius of curvature $R_0$ is also a parameter of the bend; along with the design energy it determines the strength of the magnetic field $B_0=B_z(R_0)$ on the design trajectory. However, we also require a third parameter, the field index $n$. The field index is defined

$$\text{(A.18)}\quad n\equiv-\frac{R_0}{B_0}\frac{\partial B_z}{\partial r}\bigg|_{r=R_0}.$$

The field index is simply the normalized derivative of the bending field evaluated at the design radius. In order to provide focusing in both transverse planes it is necessary that the bending field decrease in the radial direction. Kerst and Serber first studied these effects for the betatron [16], they found for focusing in both transverse planes it is necessary that $0<n<1$.

To find the transfer matrix for a bending magnet we start with the equations of motion in cylindrical coordinates. Since magnetic fields cannot accelerate, $\gamma$ is constant. We also assume that there is no magnetic field in the $\theta$ direction. With these considerations the equations of motion are

$$\begin{aligned}\gamma m\ddot{r}-\gamma mr\dot{\theta}^2&=qr\dot{\theta}B_z,\\ \gamma mr\ddot{\theta}+2\gamma m\dot{r}\dot{\theta}&=q\dot{z}B_r-q\dot{r}B_z,\\ \gamma m\ddot{z}&=-qr\dot{\theta}B_r.\end{aligned}\qquad\text{(A.19)}$$

The first-order variation in both magnetic field components $B_r$ and $B_z$ can be written in terms of the field index $n$ using the fact that $\nabla\times\mathbf{B}=0$. We have

$$
\begin{aligned}
B_z &= B_0 - nB_0\frac{r-R_0}{R_0}, \\
B_r &= -nB_0\frac{z}{R_0},
\end{aligned}
\tag{A.20}
$$

where we have assumed that $B_r(z=0)=0$ by design. Now we assume a perturbation around the design trajectory according to

$$
\begin{aligned}
r &= R_0 + \varepsilon x + O(\varepsilon^2), \\
\theta &= \omega_c t + \varepsilon\frac{z}{R_0} + O(\varepsilon^2), \\
z_{cyl} &= \varepsilon y + O(\varepsilon^2),
\end{aligned}
\tag{A.21}
$$

where $\varepsilon<<1$ is a dimensionless parameter used to keep track of the order of approximation. Note that we have identified the cylindrical coordinate $z$ with subscript *cyl* whereas the beam coordinate $z$ is unadorned. Note also that the path length parameter $s$ is related to $\theta$ by

$$
s = R_0(\alpha - \omega_c t) \qquad \Rightarrow \qquad \frac{d}{dt} = -\omega_c R_0\frac{d}{ds}. \tag{A.22}
$$

Also we have the convenient physical relations

$$
\begin{aligned}
\omega_c &\equiv \frac{qB_0}{\gamma m}, \\
v &= \frac{ds}{dt} = \dot{\theta}R_0 = \omega_c R_0, \\
B_0 &= \frac{\gamma m v}{qR_0} = \frac{\beta\gamma mc}{qR_0},
\end{aligned}
\tag{A.23}
$$

where $\omega_c$ is the cyclotron frequency.

The transfer matrix solution to the above linear perturbation is given as follows:

$$
\begin{aligned}
\mathbf{\Phi_{xx}} &= \begin{pmatrix} \cos k_x\Delta s & \frac{1}{k_x}\sin k_x\Delta s \\ -k_x\sin k_x\Delta s & \cos k_x\Delta s \end{pmatrix} \qquad \mathbf{\Phi_{yy}} = \begin{pmatrix} \cos k_y\Delta s & \frac{1}{k_y}\sin k_y\Delta s \\ -k_y\sin k_y\Delta s & \cos k_y\Delta s \end{pmatrix} \\
\mathbf{\Phi_{zz}} &= \begin{pmatrix} 1 & -\frac{k_x\beta^2\Delta s - \sin k_x\Delta s}{k_x^3 R_0^2} + \left(1 - \frac{1}{k_x^2 R_0^2}\right)\Delta s \\ 0 & 1 \end{pmatrix}
\end{aligned}
\tag{A.24}
$$

In addition, we also have the off-diagonal blocks

$$
\mathbf{\Phi_{xz}} = \begin{pmatrix} 0 & \frac{R_0\left(1-\cos k_x\Delta s\right)}{k_x^2} \\ 0 & \frac{R_0\sin k_x\Delta s}{k_x} \end{pmatrix} \qquad \mathbf{\Phi_{zx}} = \begin{pmatrix} -\frac{R_0\sin k_x\Delta s}{k_x} & \frac{R_0\left(1-\cos k_x\Delta s\right)}{k_x^2} \\ 0 & 0 \end{pmatrix} \tag{A.25}
$$

where

$$k_x = \frac{\sqrt{1-n}}{R_0},$$

(A.26) $$k_y = \frac{\sqrt{n}}{R_0},$$

$$\Delta s = \alpha R_0 .$$

The above description is for a bend in the horizontal plane to the right (positive $x$ direction). For a bend to the left replace $\mathbf{\Phi_{xz}}$ and $\mathbf{\Phi_{zx}}$ by $-\mathbf{\Phi_{xz}}$ and $-\mathbf{\Phi_{zx}}$, respectively.

### A.6 RF Gap (As a Thin Lens)

Here we treat the effects of a general RF gap as a thin lens. The energy gain in the gap $\Delta W$ is given in terms of the Panofsky equation [25]

(A.27) $$\Delta W = qE_0 TL\cos\phi ,$$

where $q$ is the unit charge, $E_0$ is the longitudinal electric field in the gap, $T$ is the transit time factor (the ratio of the energy gained in the RF gap to that of a DC gap of the same field amplitude), and $\phi$ is the RF phase of the synchronous particle at the center of the gap. Along with $h$, the (integer) number of the field harmonic, we assume that these are the parameters of the RF gap.

The electric fields in the gap cause longitudinal focusing and radial defocusing, as well as the change in energy. Here we present the thin lens focusing constants to account for these effects. The values of $x'$, $y'$ and $z'$ tend to decrease with increasing longitudinal momentum simply because they are normalized by this quantity. However, the unnormalized values $p_x$, $p_y$, and $\Delta p$ are constant with an increase in longitudinal momentum. Thus, the action of the RF gap is produced by first unnormalizing the momentum components, transforming by a thin lens, then normalizing the momentum components with respect to the new, larger longitudinal momentum. For example, for the $x$ phase plane we have

$$p_{x,n} = p_i x'_n = (\beta\gamma)_i mc\, x'_n ,$$

(A.28) $$p_{x,n+1} = p_{x,n} + k_x x_n ,$$

$$x'_{n+1} = \frac{p_{x,n+1}}{p_f} = \frac{p_{x,n+1}}{(\beta\gamma)_f mc},$$

where the subscript $i$ refers to quantities with initial energy and the subscript $f$ refers to quantities with the final energy. The following transfer matrix captures this sequence of operations:

$$\mathbf{\Phi_{xx}} = \begin{pmatrix} 1 & 0 \\ 0 & \dfrac{1}{(\beta\gamma)_f mc} \end{pmatrix} \begin{pmatrix} 1 & 0 \\ k_x & 1 \end{pmatrix} \begin{pmatrix} 1 & 0 \\ 0 & (\beta\gamma)_i mc \end{pmatrix},$$

(A.29)

$$= \begin{pmatrix} 1 & 0 \\ \dfrac{1}{(\beta\gamma)_f}\dfrac{k_x}{mc} & \dfrac{(\beta\gamma)_i}{(\beta\gamma)_f} \end{pmatrix}.$$

Likewise, for the other phase planes we have

$$\mathbf{\Phi_{yy}} = \begin{pmatrix} 1 & 0 \\ \dfrac{1}{(\beta\gamma)_f}\dfrac{k_y}{mc} & \dfrac{(\beta\gamma)_i}{(\beta\gamma)_f} \end{pmatrix}$$

(A.30)

$$\mathbf{\Phi_{zz}} = \begin{pmatrix} 1 & 0 \\ \dfrac{\bar{\gamma}^2}{\gamma_f^2(\beta\gamma)_f}\dfrac{k_z}{mc} & \dfrac{\gamma_i^2(\beta\gamma)_i}{\gamma_f^2(\beta\gamma)_f} \end{pmatrix},$$

Note that

$$
\begin{aligned}
(\beta\gamma)_i &= \sqrt{\gamma_i^2 - 1}, \\
(\beta\gamma)_f &= \sqrt{\gamma_f^2 - 1}, \\
\gamma_{i,f} &= 1 + \frac{W_{i,f}}{E_R}, \\
W_f &= W_i + \Delta W,
\end{aligned}
\tag{A.31}
$$

where $E_R$ is the rest energy of the beam particle ($mc^2$). The values of the focusing coefficients are found by integrating the electromagnetic fields in the gap. We have (approximately, for example see [25])

$$
\frac{k_x}{mc} = \frac{k}{mc}, \qquad \frac{k_y}{mc} = \frac{k}{mc}, \qquad \frac{k_z}{mc} = -2\bar{\gamma}^2 \frac{k}{mc},
\tag{A.32}
$$

where

$$
\frac{k}{mc} \equiv h \frac{\pi}{\bar{\beta}^2 \bar{\gamma}^2 mc^2 \lambda} qE_0 L \sin(-\phi),
\tag{A.33}
$$

$\bar{\beta}, \bar{\gamma}$ are the relativistic parameters evaluated at the average energy

$$
\bar{W} = W_i + \Delta W / 2,
\tag{A.34}
$$

and $h$ is the field harmonic at which the gap is operating.

If the longitudinal coordinates are given as ($z$,$\Delta p/p$) the corresponding transfer block is then

$$
\mathbf{\Phi_{zz}} = \begin{pmatrix} 1 & 0 \\ \dfrac{1}{(\beta\gamma)_f} \dfrac{k_z}{mc} & \dfrac{(\beta\gamma)_i}{(\beta\gamma)_f} \end{pmatrix}.
\tag{A.35}
$$

This value may be used to approximate the previous matrix since $\bar{\gamma}^2 / \gamma^2$ is typically close to unity.

## APPENDIX B: 2D PHASE SPACE MOMENT CALCULATIONS

The moments of a distribution described by Eq. **Error! Reference source not found.** may be computed using a technique similar to that of Dragt et al [9]. Specifically, let

$$\text{(B.1)} \qquad \left\langle q^m p^n \right\rangle = \frac{1}{N} \int_{-\infty-\infty}^{+\infty+\infty} q^m p^n f\left[z^T Q z\right] d^2 z \,,$$

where

$$\text{(B.2)} \qquad N = \int_{-\infty-\infty}^{+\infty+\infty} f\left[z^T Q z\right] d^2 z, \quad Q \equiv \begin{pmatrix} \gamma & \alpha \\ \alpha & \beta \end{pmatrix}, \qquad z \equiv \begin{pmatrix} q \\ p \end{pmatrix} \quad \text{and} \quad d^2 z \equiv dq\, dp \,.$$

The matrix $Q$ is symmetric and positive definite. Thus, there is an $R \in SO(2)$ which diagonalizes $Q$, say

$$\text{(B.3)} \qquad \Lambda = R^T Q R = \begin{pmatrix} \lambda_1 & 0 \\ 0 & \lambda_2 \end{pmatrix},$$

where $\lambda_1$, $\lambda_2$ are the eigenvalues of $Q$. Note that

$$\text{(B.4)} \qquad \det \Lambda = \lambda_1 \lambda_2 = \det Q = \beta\gamma - \alpha^2 = 1 \,,$$

where the last relation is a property of the Courant-Snyder parameters. With the substitution $\zeta = R^T z$ and the fact that $\det R = 1$, we have

$$\text{(B.5)} \qquad \left\langle q^m p^n \right\rangle = \frac{1}{N} \int_{-\infty-\infty}^{+\infty+\infty} (R_{11}\zeta_1 + R_{12}\zeta_2)^m (R_{21}\zeta_1 + R_{22}\zeta_2)^n f\left[\zeta^T \Lambda \zeta\right] d^2 \zeta \,,$$

Using the additional substitution

$$\text{(B.6)} \qquad \zeta_1 = \frac{r}{\sqrt{\lambda_1}} \cos\theta, \quad \zeta_2 = \frac{r}{\sqrt{\lambda_2}} \sin\theta, \quad d^2\zeta = \frac{r\, dr\, d\theta}{\sqrt{\lambda_1 \lambda_2}} = r\, dr\, d\theta \,,$$

we obtain the formula

$$\text{(B.7)} \qquad \left\langle q^m p^n \right\rangle = \frac{F_{\frac{m+n}{2}}}{F_0} \frac{1}{2\pi} \int_0^{2\pi} \left( \frac{R_{11}}{\sqrt{\lambda_1}} \cos\theta + \frac{R_{12}}{\sqrt{\lambda_2}} \sin\theta \right)^m \left( \frac{R_{21}}{\sqrt{\lambda_1}} \cos\theta + \frac{R_{22}}{\sqrt{\lambda_2}} \sin\theta \right)^n d\theta \,,$$

where

$$\text{(B.8)} \qquad F_k \equiv \int_0^\infty s^k f(s)\, ds \,.$$

The above formula can be used to compute all the moments and, thus, the kinematic invariants, in terms of the $F_k$.

## APPENDIX B: NOTES ON THE SPECIAL ORTHOGONAL GROUPS SO(2) AND SO(3)

The special orthogonal group in two dimensions, denoted $SO(2)$, is the mathematical group of rotations of the plane. It has the topology of the circle $S^1$ and is the simplest closed Lie group. It may be represented as the circle in the complex plane $\{e^{i\theta} \in | \theta \in [0,2\pi)\}$, or we may use the matrix representation

$$SO(2) = \left\{ \mathbf{R}(\theta) \equiv \begin{pmatrix} \cos\theta & -\sin\theta \\ \sin\theta & \cos\theta \end{pmatrix} \in SL(2,\Re) \;\middle|\; \theta \in [0,2\pi) \right\}, \tag{B.1}$$

where $SL(2,\Re)$ is the special linear group, specifically, the group of 2×2 real matrices with determinant one. Note that the matrices $\mathbf{R}(\theta)$ act on points $(x\ y)$ of the plane as a counter-clockwise rotation. We have the group behavior $\mathbf{R}(\theta_1)\mathbf{R}(\theta_2)=\mathbf{R}(\theta_1+\theta_2 \bmod 2\pi)$ so that $SO(2)$ is seen to be a one-parameter group. From the form of the $\mathbf{R}(\theta)$ we also see that $\mathbf{R}(-\theta)=\mathbf{R}^T(\theta)=\mathbf{R}^{-1}(\theta)$. The generator of this group is the matrix

$$\mathbf{L} = \begin{pmatrix} 0 & -1 \\ 1 & 0 \end{pmatrix}, \tag{B.2}$$

so that any matrix $\mathbf{R}(\theta) \in SO(2)$ is generated according to

$$\mathbf{R}(\theta) = e^{\theta \mathbf{L}}. \tag{B.3}$$

Note that the matrix $\mathbf{L} \in SL(2,\Re)$ has similar properties to the imaginary unit $i$ of the complex numbers , specifically, $\mathbf{L}^2=-\mathbf{1}$.

Any symmetric 2×2 matrix $\mathbf{M} = \begin{pmatrix} \gamma & \alpha \\ \alpha & \beta \end{pmatrix}$ may be diagonalized through conjugation by some element $\mathbf{R}(\theta)$ of $SO(2)$. It is straightforward to determine $\theta$ in this case. Consider the following:

$$\begin{aligned} \mathbf{R}(\theta)\mathbf{M}\mathbf{R}^T(\theta) &= \begin{pmatrix} \cos\theta & -\sin\theta \\ \sin\theta & \cos\theta \end{pmatrix} \begin{pmatrix} \gamma & \alpha \\ \alpha & \beta \end{pmatrix} \begin{pmatrix} \cos\theta & \sin\theta \\ -\sin\theta & \cos\theta \end{pmatrix} \\ &= \begin{pmatrix} \gamma\cos^2\theta - 2\alpha\sin\theta\cos\theta + \beta\sin^2\theta & \dfrac{\gamma-\beta}{2}\sin 2\theta + \alpha\cos 2\theta \\ \dfrac{\gamma-\beta}{2}\sin 2\theta + \alpha\cos 2\theta & \beta\cos^2\theta + 2\alpha\sin\theta\cos\theta + \gamma\sin^2\theta \end{pmatrix} \end{aligned} \tag{B.4}$$

By choosing

$$\theta = \frac{1}{2}\tan^{-1}\frac{2\alpha}{\beta-\gamma}, \tag{B.5}$$

the off-diagonal elements of the above matrix become zero thus diagonalizing $M$.

The special orthogonal group in three dimensions, $SO(3)$, is the group of rigid-body rotations in Euclidean three-space. It can be represented by the set of 3×3 matrices, with determinant one, which preserve the Euclidean inner product in $\Re^3$. That is,

$$SO(3) = \left\{ \mathbf{M} \in GL(3,\Re) \,|\, \mathbf{M}\mathbf{M}^T = \mathbf{1}, \det(\mathbf{M}) = 1 \right\}. \tag{B.6}$$

From the matrix form of $\mathbf{R}(\theta)$ above, we can immediately identify three special one-parameter subgroups of SO(3). Namely, they are the sets of counter-clockwise rotations around the $x,y,z$ coordinate axes, which we denote $\mathbf{R}_x(\alpha)$, $\mathbf{R}_y(\beta)$, $\mathbf{R}_z(\gamma)$, respectively. They are

$$\mathbf{R}_{\mathbf{x}}(\alpha) \equiv \begin{pmatrix} 1 & 0 & 0 \\ 0 & \cos\alpha & -\sin\alpha \\ 0 & \sin\alpha & \cos\alpha \end{pmatrix},$$

$$\mathbf{R}_{\mathbf{y}}(\beta) \equiv \begin{pmatrix} \cos\beta & 0 & \sin\beta \\ 0 & 1 & 0 \\ -\sin\beta & 0 & \cos\beta \end{pmatrix}, \quad \text{(B.7)}$$

$$\mathbf{R}_{\mathbf{z}}(\gamma) \equiv \begin{pmatrix} \cos\gamma & -\sin\gamma & 0 \\ \sin\gamma & \cos\gamma & 0 \\ 0 & 0 & 1 \end{pmatrix},$$

where $\alpha,\beta,\gamma \in [0,2\pi)$. Although $SO(3)$ is a three-parameter group and the set $\{\mathbf{R}_{\mathbf{x}}(\alpha),\mathbf{R}_{\mathbf{y}}(\beta),\mathbf{R}_{\mathbf{z}}(\gamma) | \alpha,\beta,\gamma \in [0,2\pi)\}$ spans $SO(3)$ [21], the above matrices are not independent. To see this note that $\mathbf{R}_{\mathbf{x}}(\theta)=\mathbf{R}_{\mathbf{y}}(-\pi/2)\mathbf{R}_{\mathbf{z}}(\theta)\mathbf{R}_{\mathbf{y}}(\pi/2)$. That is, a rotation $\theta$ about the $x$ axis can be generated by a backward quarter-rotation about the $y$ axis, a rotation $\theta$ about the $z$ axis, followed by a forward quarter-rotation about the $y$ axis.

The generators of the above one-parameter groups are

$$\mathbf{L}_{\mathbf{x}} \equiv \begin{pmatrix} 0 & 0 & 0 \\ 0 & 0 & -1 \\ 0 & 1 & 0 \end{pmatrix},$$

$$\mathbf{L}_{\mathbf{y}} \equiv \begin{pmatrix} 0 & 0 & 1 \\ 0 & 0 & 0 \\ -1 & 0 & 0 \end{pmatrix}, \quad \text{(B.8)}$$

$$\mathbf{L}_{\mathbf{z}} \equiv \begin{pmatrix} 0 & -1 & 0 \\ 1 & 0 & 0 \\ 0 & 0 & 0 \end{pmatrix},$$

so that $\mathbf{R}_{\mathbf{x}}(\alpha) = e^{\alpha \mathbf{L}_{\mathbf{x}}}$, $\mathbf{R}_{\mathbf{y}}(\beta) = e^{\beta \mathbf{L}_{\mathbf{y}}}$, and $\mathbf{R}_{\mathbf{z}}(\gamma) = e^{\gamma \mathbf{L}_{\mathbf{z}}}$.

## APPENDIX C: SELF-FIELD MOMENT CALCULATION

We shall calculate the moment $\langle zE_z \rangle$. The other field moments follow a similar procedure.

$$\text{(C.1)} \qquad \left\langle zE_z \right\rangle = \frac{1}{N}\iiint z\left[-\frac{\partial\phi(x,y,z)}{\partial z}\right]F\left(\frac{x^2}{a^2}+\frac{y^2}{b^2}+\frac{z^2}{c^2}\right)dxdydz\,.$$

Substituting the value for potential $\phi$ from Eq. (107) we have

$$\text{(C.2)} \quad \left\langle zE_z \right\rangle = \frac{1}{N}\frac{qabc}{2\varepsilon_0}\int_{-\infty}^{+\infty}\int_{-\infty}^{+\infty}\int_{-\infty}^{+\infty}\int_0^{\infty} z^2 \frac{F\left(\frac{x^2}{t+a^2}+\frac{y^2}{t+b^2}+\frac{z^2}{t+c^2}\right)}{(t+a^2)^{1/2}(t+b^2)^{1/2}(t+c^2)^{3/2}}F\left(\frac{x^2}{a^2}+\frac{y^2}{b^2}+\frac{z^2}{c^2}\right)dtdxdydz\,.$$

Since the integrations are independent we may switch the order so the integration with respect to $t$ is last. Now employ the change of coordinates

$$\text{(C.3)} \qquad \begin{aligned} x &= r\sqrt{t+a^2}\,\sin\theta\cos\phi \\ y &= r\sqrt{t+b^2}\,\sin\theta\sin\phi \qquad dxdydz = \sqrt{t+a^2}\,\sqrt{t+b^2}\,\sqrt{t+c^2}\,r^2\sin\theta \\ z &= r\sqrt{t+c^2}\,\cos\theta \end{aligned}$$

along with the appropriate limits of integration to yield

$$\text{(C.4)} \qquad \left\langle zE_z \right\rangle = \frac{1}{N}\frac{qabc}{2\varepsilon_0}\int_0^{\infty}\int_0^{2\pi}\int_0^{\pi}\int_0^{\infty} r^2\cos^2\theta F(r^2)F\left[r^2+tr^2u(\theta,\phi)\right]r^2\sin\theta dr d\theta d\phi dt\,,$$

where the function $u(\theta,\phi)$ is defined

$$\text{(C.5)} \qquad u(\theta,\phi) \equiv \sin^2\theta\left(\frac{\cos^2\phi}{a^2}+\frac{\sin^2\phi}{b^2}\right)+\frac{\cos^2\theta}{c^2}\,.$$

We now switch the order of integration again and apply the substitution

$$\text{(C.6)} \qquad \tau = r^2+tr^2u(\theta,\phi) \qquad dt = \frac{d\tau}{r^2u(\theta,\phi)}$$

to produce

$$\text{(C.7)} \qquad \left\langle zE_z \right\rangle = \frac{1}{N}\frac{qabc}{2\varepsilon_0}\int_0^{2\pi}\int_0^{\pi}\frac{\cos^2\theta\sin\theta}{u(\theta,\phi)}d\theta d\phi\int_0^{\infty}\int_{r^2}^{\infty} r^2F(r^2)F(\tau)d\tau dr\,.$$

Using the definitions

$$\text{(C.8)} \qquad G(r) \equiv \int_r^{\infty} F(s)ds \qquad \text{and} \qquad \Gamma(F) \equiv \int_0^{\infty} G^2(r^2)dr\,,$$

and the fact that

$$\text{(C.9)} \qquad \int_0^{\infty} r^2F(r^2)G(r^2)dr = \frac{1}{4}\Gamma(F)\,,$$

the original integration is reduced to

$$\text{(C.10)} \quad \left\langle zE_z \right\rangle = \frac{\Gamma(F)}{N}\frac{qabc}{8\varepsilon_0}\int_0^{2\pi}\int_0^{\pi}\frac{\cos^2\theta\sin\theta}{u(\theta,\phi)}d\theta d\phi$$

where we have integrated out the distribution dependence.

Note that the function $u(\theta,\phi)$ can be written

$$u(\theta,\phi)=\left[\frac{a^2+b^2}{2a^2b^2}\sin^2\theta+\frac{1}{c^2}\cos^2\theta\right]+\left[\frac{b^2-a^2}{2a^2b^2}\sin^2\theta\right]\cos 2\phi\,. \tag{C.11}$$

Using this decomposition and the fact that

$$\int_0^{2\pi}\frac{d\phi}{A+B\cos 2\phi}=\frac{2\pi}{\sqrt{A^2-B^2}}\,, \tag{C.12}$$

further reduces Eq. (C.10) to

$$\begin{aligned}\left\langle zE_z\right\rangle &= \frac{\Gamma(F)}{N}\frac{q\pi}{4\varepsilon_0}abc\int_0^{\pi}\frac{\cos^2\theta\sin\theta}{\left[\dfrac{\sin^4\theta}{a^2b^2}+\left(\dfrac{1}{a^2}+\dfrac{1}{b^2}\right)\dfrac{\sin^2\theta\cos^2\theta}{c^2}+\dfrac{\cos^4\theta}{c^4}\right]^{1/2}}d\theta \\ &= \frac{\Gamma(F)}{N}\frac{q\pi}{4\varepsilon_0}abc\int_0^{\pi}\frac{\cos^2\theta\sin\theta}{\left(\dfrac{\sin^2\theta}{a^2}+\dfrac{\cos^2\theta}{c^2}\right)^{1/2}\left(\dfrac{\sin^2\theta}{b^2}+\dfrac{\cos^2\theta}{c^2}\right)^{1/2}}d\theta\end{aligned} \tag{C.13}$$

If we employ the substitution

$$\cos\theta=\frac{c}{\sqrt{t+c^2}}\qquad \sin\theta=\sqrt{\frac{t}{t+c^2}}\qquad \sin\theta d\theta=\frac{1}{2}\frac{c}{\left(t+c^2\right)^{3/2}}dt \tag{C.14}$$

we find that

$$\left\langle zE_z\right\rangle=\frac{\Gamma(F)}{N}\frac{q\pi a^2b^2c^2}{4\varepsilon_0}c^2\int_0^{\infty}\frac{dt}{(t+a^2)^{1/2}(t+b^2)^{1/2}(t+c^2)^{3/2}}dt\,. \tag{C.15}$$

or

$$\left\langle zE_z\right\rangle=\frac{\Gamma(F)}{N}\frac{q\pi a^2b^2c^2}{6\varepsilon_0}c^2R_D[a^2,b^2,c^2]\,, \tag{C.16}$$

where $R_D$ is the Carlson elliptic integral of the second kind.

## REFERENCES


[1] C.K. Allen, "Bunched Beam Envelope Equations Including Image Effects from a Cylindrical Pipe", Phys. Rev. E, Vol. 55, No. 6-B (1997), pp. 7591-7605.

[2] C.K. Allen and N. Pattengale, "Theory and Technique of Beam Envelope Simulation" LANL internal report LA-UR-02-4979.

[3] H. Anton, *Elementary Linear Algebra, Fourth Edition* (Wiley, New York, 1984), Sect. 7.3-7.4.

[4] D.C. Carey, K.L. Brown and F. Rothacker, *Third-Order TRANSPORT - A Computer Program for Designing Charged Particle Beam Transport Systems*, Stanford Linear Accelerator Center Report No. SLAC-R-95-462 (1995).

[5] B.C. Carlson, *SIAM Journal on Mathematical Analysis*, Vol. 8 (1977), pp. 231-242.

[6] B.C. Carlson, *Math. Comp.*, Vol. 49 (1987), pp. 595-606.

[7] K.R. Crandall and D.P. Rusthoi, *Trace 3-D Documentation, Third Edition*, Los Alamos Code Group LA-UR-97-886 (May, 1997).

[8] C.N. Dorny, *A Vector Space Approach to Models and Optimization* (Krieger Publishing, Malabar, FL, 1980 - original publication by Wiley, 1975), Chapt. 5.

[9] A.J. Dragt, R.L. Gluckstern, F. Neri, and G. Rangarajan, "Theory of Emittance Invariants", *Frontiers of Particle Beams; Observation, Diagnosis and Correction*, Lecture Notes in Physics 343, edited by M. Month and S. Turner (Springer-Verlag, Berlin, 1988), pp. 94-121.

[10] See any introductory text on ordinary differential equations such as E.A. Coddington and N. Levinson, *Theory of Ordinary Differential Equations* (McGraw-Hill, New York, 1955).

[11] R.L. Gluckstern, "Scalar Potential for Charge Distributions with Ellipsoidal Symmetry", Fermilab Internal Report TM-1402 (1986).

[12] D.D. Holm, W.P. Lysenko, and J.C. Scovel, "Moment Invariants of the Vlasov Equation", *J. Math. Phys.*, Vol. 31, No. 7 (July, 1990), pp. 1610-1615.

[13] P.M. Lapostolle, CERN report AR/Int. SG/65-15, Geneva, Switzerland (July, 1965).

[14] W.P. Lysenko and M. Overley, "Moment Invariants for Particle Beams", *Linear Accelerators and Beam Optics Codes*, AIP Conference Proceedings 177, edited by C.R. Eminhizer (AIP, New York, 1988), pp. 323-335.

[15] O.D. Kellogg, *Foundations of Potential Theory* (Dover, 1953) pp. 192-194.

[16] D.W. Kerst and R. Serber, *Phys Rev.* **60**, 53 (1941).

[17] D.G. Luenberger, *Optimization by Vector Space Methods* (Wiley, New York, 1969), Chapt. 4.

[18] N.D. Pattengale and C.K. Allen, "The Software Anatomy of a Flexible Accelerator Simulation Engine", Los Alamos National Laboratory Internal Report LA-UR-02-3761.

[19] W.H. Press, S.A. Teukolsky, W.T. Vetterling, and B.P. Flannery, *Numerical Recipes in C, Second Edition* (Cambridge University Press, Cambridge, 1992), pp. 261-269.

[20] W. Schroeder, K. Martin, and B. Lorensen, *The Visualization Toolkit, Second Edition* (Prentice Hall, Upper Saddle River, NJ, 1998), Section 3.7.

[21] D.H. Sattinger and O.L. Weaver, Lie Groups and Algebras with Applications to Physics, Geometry, and Mechanics (Springer-Verlag, New York, 1986).

[22] F.R. Sacherer, "RMS Envelope Equations with Space Charge", *IEEE Trans. Nucl. Sci.*, Vol. NS-18 (1971), pp. 1105-1107.

[23] I. Stakgold, *Green's Functions and Boundary Value Problems* (Wiley, New York, 1979), pp. 210-214.

[24] M. Reiser, *Theory and Design of Charged Particle Beams* (Wiley, New York, 1994), Chapt. 4, p. 151, p. 196, p. 359.

[25] T.P. Wangler, *RF Linear Accelerators* (Wiley, New York, 1998), Chapt. 9, p. 278.